Pergamon

Int. J. Solids Structures Vol. 31, No. 20, pp. 2769–2792, 1994

0020–7683/94 $7.00 + .00

0020-7683(94)E0057-3

DOUBLY CONSTRAINED ELASTIC WAVE PROPAGATION

G. A. ROGERSON
Mathematics and Computing Section, Department of Applied Science, University College Salford, Salford M6 6PU, U.K.

and

N. H. SCOTT
School of Mathematics, University of East Anglia, Norwich NR4 7TJ, U.K.

(*Received* 19 *November* 1993; *in revised form* 28 *March* 1994)

Abstract—It is well known that an elastic material subject to N ($0 \leqslant N \leqslant 3$), internal constraints upon the deformation gradient admits the propagation of $3-N$ distinct plane waves in most directions. Those directions in which more than $3-N$ waves may propagate are termed *exceptional*. Here we investigate wave propagation in a material subject to two constraints by slightly relaxing both constraints and asymptotically expanding the wave speeds and the polarizations in inverse powers of the large elastic moduli associated with the slightly relaxed constraints. The limits in which (1) both constraints operate exactly, and (2) one constraint is exact and one slightly relaxed are both discussed and shown to confirm previous results. The theory and graphical illustrations of the slowness surface are presented for two examples of a practical nature: (1) an incompressible material reinforced by a set of parallel inextensible fibres; (2) a material reinforced by two sets of mutually orthogonal inextensible fibres.

1. INTRODUCTION

In recent years various mathematical models have been developed to aid fundamental understanding of the mechanical and dynamical properties of various engineering materials. In order to keep the models mathematically tractable, whilst still describing the important physical characteristics of the elastic or plastic material being modelled, internal constraints have been extensively employed. An internal constraint is a restriction upon the possible deformations that a material may undergo and as such is a mathematical idealization which reduces the complexity of the governing equations for any particular problem. This technique yields a solution which is the leading order solution of a perturbation method which may be used to examine an associated unconstrained problem in which the constraint is taken to be operating approximately in a sense to be made explicit. For example, Ericksen (1986) has described aspects of the behaviour of twinned crystals by introducing constraints such as a restriction in shear and the constancy of the trace of the right Cauchy–Green strain tensor whilst Scott (1992a) relaxed these constraints slightly in a study of plane wave propagation in twinned crystals. The constancy of the sum of the principal stretches, the so-called Bell constraint, was developed by Bell (1985, 1989) in the context of finite-strain plasticity theory, and has also been discussed in the context of finite elasticity [see Beatty and Hayes (1992a, b); Willson and Myers (1990)]. In addition, recent continuum models developed to describe smectic C liquid crystals have essentially used internal constraints. For these classes of liquid crystals the constraints employed are not all homogeneous [see e.g. Stewart and Raj (1990), eqn (2.2)].

Although a certain amount of attention has been focused upon the constraints mentioned in the preceding paragraph, the two most commonly encountered constraints remain those of incompressibility and inextensibility in a specified direction. The first of these may be used to model a solid with a bulk modulus much larger than any other elastic modulus, e.g. rubber-like materials, whilst the second may be used to model fibre-reinforced composites with a large Young's modulus in the fibre direction. The usual idealized model for

a fibre-reinforced composite is then an elastic solid transversely isotropic about an inextensible fibre direction. The further imposition of the constraint of incompressibility is sometimes made and the resulting solid is usually referred to as the idealized fibre-reinforced material (IFRM) [see Spencer (1972)].

Although the use of internal constraints does lead to greatly simplified models certain singular behaviour occurs, particularly in relation to wave propagation, and has to be carefully interpreted. When N ($\leqslant 3$) internal constraints are imposed on an elastic solid, $3-N$ plane waves propagate in each non-exceptional direction, an exceptional direction being one for which the number of fully active constraints is less than N [see e.g. Chadwick *et al.* (1985)]. This situation is in contrast to the classical result in the unconstrained case where three plane waves propagate in each direction [see Truesdell and Noll (1965)]. The fact that the number of waves able to propagate in a constrained elastic solid is a discontinuous function of propagation direction is clearly to be regarded as unphysical. This singular behaviour has been discussed in the case of the single constraint of inextensibility by Green (1978). Scott (1986) has discussed the single constraint of incompressibility, for which no exceptional directions occur. Rogerson and Scott (1992a) have extended the analysis of the previous two authors to discuss the effects on wave propagation of a single constraint of arbitrary nature. By slightly relaxing the constraint, these authors show that in the neighbourhood of any exceptional direction rapid changes occur to one of the wave speeds. In the constrained limit this speed becomes infinite in every direction other than the exceptional ones, in which the wave speed retains finite magnitude. As the material approaches the constrained limit the wave with infinite speed is conjectured to become unwavelike, with zero amplitude and infinite wavelength. This has been shown to be the case for a limited class of traction boundary value problems for incompressible and inextensible half-spaces by Rogerson and Scott (1992b) who obtained their results by inverting integral transform solutions. An indefinitely growing wave speed may be thought of as an indication of increasing material rigidity.

For the problem of wave propagation in a singly constrained elastic solid, an exceptional direction occurs when a certain vector function of the wave normal, usually called the constraint vector, vanishes (see Section 2.2 below). In multi-constrained wave problems things become more complicated with exceptional directions occurring when the associated constraint vectors fail to be linearly independent. For example, Rogerson and Scott (1991) show that seven distinct classes of exceptional direction occur when an elastic body is subjected to three internal constraints.

In this paper we consider the propagation of waves in a doubly constrained elastic solid for which the two constraints are relaxed slightly. The methodology employed involves seeking perturbation expansions for the wave speeds and polarization vectors essentially in inverse powers of the large elastic moduli which characterize each constraint. An alternative approach adopted recently by Rogerson and Scott (1993) involves imposing one constraint exactly whilst relaxing the other. This method has the advantage that the two wave speeds satisfy a quadratic equation, rather than a cubic, and so are obtainable in explicit form. However, this method has its drawbacks as the limit is dependent upon which constraint is imposed exactly and which is relaxed. This is clearly seen if the results for an inextensible, nearly incompressible material are compared with those for an incompressible, nearly inextensible material [see Rogerson and Scott (1993) and Scott (1992b), respectively]. The method employed in this paper therefore offers a far more robust method of elucidating the limiting behaviour of a doubly constrained elastic solid.

In Section 2 we begin by reviewing the classical theory of wave propagation in unconstrained elastic solids. This section continues with a discussion of arbitrarily constrained elastic wave propagation and concludes with the introduction of the concept of an arbitrary near-constraint. The broad theoretical framework developed in Section 2 is specialized in the next section to discuss the problem of waves propagating in a doubly constrained solid. Three classes of exceptional direction occur and are fully discussed. The two constraints are relaxed in Section 4 and perturbation schemes for the squared wave speeds and associated polarization vectors are set up and solved. The propagation of waves in the neighbourhood of the three classes of exceptional direction known to occur in the doubly constrained solid

is examined in some detail in Section 5. The paper continues in Section 6 with a discussion of two examples involving the constraints of incompressibility and inextensibility. The first of these concerns an incompressible elastic body reinforced by a set of inextensible fibres whilst the second concerns a compressible elastic solid reinforced by two mutually orthogonal sets of inextensible fibres. Both of these examples are illustrated graphically by means of a presentation of various cross-sections of the appropriate slowness surfaces. These plots also illustrate the limiting process.

2. BASIC EQUATIONS

We consider a homogeneous elastic body B which, when unstressed, occupies a region B_u in three-dimensional Euclidean space. In this reference state a material particle has Cartesian position vector $\mathbf{X}$ relative to some arbitrarily chosen origin. Let us suppose that B undergoes a homogeneous finite static deformation to an equilibrium state B_e in which the point $\mathbf{X}$ takes up the new position $\mathbf{x}(\mathbf{X})$, with respect to the same coordinate frame. The deformation gradient and left and right Cauchy–Green strain tensors are defined by the constant tensors

$$F_{iA} = \frac{\partial x_i}{\partial X_A}, \quad \mathbf{B} = \mathbf{F}\mathbf{F}^{\mathrm{T}}, \quad \mathbf{C} = \mathbf{F}^{\mathrm{T}}\mathbf{F}, \tag{1}$$

respectively, and the Jacobian of the transformation is denoted by

$$J = \det \mathbf{F}. \tag{2}$$

2.1. *Unconstrained materials*

According to the principal of objectivity the strain energy function per unit volume of reference configuration is a function of the right Cauchy–Green strain tensor. The Cauchy stress is therefore representable in the component form

$$\sigma^{\mathrm{c}}_{ij} = 2J^{-1}F_{iA}F_{jB}\frac{\partial W^{\mathrm{c}}}{\partial C_{AB}}, \tag{3}$$

where $W^{\mathrm{c}}(\mathbf{C})$ is the strain energy function and the superscript c is used to denote components arising purely from the deformation, i.e. the constitutive components. For unconstrained materials there is clearly no necessity to indicate explicitly the constitutive components but the motivation for introducing such notation will become clear during later discussions concerning constrained solids. The fourth-order tensor of elastic moduli is defined by

$$d^{\mathrm{c}}_{ijkl} = 2J^{-1}\delta_{ik}F_{jA}F_{lB}\frac{\partial W^{\mathrm{c}}}{\partial C_{AB}} + 4J^{-1}F_{iA}F_{jB}F_{kC}F_{lD}\frac{\partial^2 W^{\mathrm{c}}}{\partial C_{AB}\partial C_{CD}}, \tag{4}$$

and possesses the symmetries $d^{\mathrm{c}}_{ijkl} = d^{\mathrm{c}}_{klij}$ but, in general, no others.

Suppose that an infinitesimal, time-varying displacement $\mathbf{u}(\mathbf{x}, t)$, taken in the form

$$\mathbf{u}(\mathbf{x}, t) = \phi(\mathbf{x}\cdot\mathbf{n} - vt)\mathbf{e}, \tag{5}$$

is superimposed upon the homogeneous prestrain $\mathbf{x}(\mathbf{X})$. Such a disturbance represents a plane wave which has a profile ϕ propagating in the direction of the real unit vector $\mathbf{n}$ with speed v and constant polarization $\mathbf{e}$. It is well known that the wave speeds v and polarization vectors $\mathbf{e}$ are obtained by solving the eigenvalue problem

$$\{\rho v^2 \mathbf{I} - \mathbf{Q}^c(\mathbf{n})\}\mathbf{e} = \mathbf{0}, \tag{6}$$

in which $\mathbf{I}$ denotes the unit tensor, ρ the density and Q^c_{ik} the components of the real symmetric acoustic tensor, defined by

$$Q^c_{ik} = d^c_{ijkl} n_j n_l \tag{7}$$

[see e.g. Truesdell and Noll (1965)].

In view of the fact that $\mathbf{Q}^c$ is a real, symmetric tensor it possesses three real eigenvalues ρv^2 for each direction of propagation $\mathbf{n}$. The three corresponding polarization vectors may be selected to be real and mutually orthogonal. Some criterion for physically realistic response, such as strong ellipticity, is usually imposed to ensure that each of the eigenvalues of eqn (6) is positive so that three homogeneous waves are able to propagate in each direction.

The slowness surface. We assume that three homogeneous waves, with speeds $v_\alpha(\mathbf{n})$, $\alpha = 1 \ldots 3$, are able to propagate in each direction $\mathbf{n}$. The slowness surface is the real three-sheeted, centro-symmetric surface formed as the locus of the vector $v_\alpha^{-1}\mathbf{n}$, $\alpha = 1 \ldots 3$, as $\mathbf{n}$ varies over the unit sphere. Musgrave (1970) has given a detailed account of the slowness surface demonstrating its importance in the theory of elastic wave propagation and giving many graphical illustrations of cross-sections of the slowness surface of naturally occurring materials. Perhaps the single most important property of the slowness surface is that at each point the normal to the surface gives the direction of propagation of the energy associated with the plane wave. We return, briefly, to the question of energy propagation at the end of Section 7.

2.2. *Constrained solids*

It is usual for problems involving internal constraints of the form $\lambda^{[A]}(\mathbf{C}) = 0$ $(A = 1 \ldots N)$ to introduce a pseudo strain energy function of the form

$$W^* = W^c + \sum_{A=1}^{N} \alpha^{[A]} \lambda^{[A]}, \tag{8}$$

with the propagation condition (6) replaced by

$$(\rho v^2 \mathbf{I} - \mathbf{Q}^*)\mathbf{e} - \sum_{A=1}^{N} q^{[A]} \mathbf{v}^{[A]} = \mathbf{0}, \quad \mathbf{v}^{[A]} \cdot \mathbf{e} = 0, \quad (A = 1 \ldots N). \tag{9}$$

In eqns (8) and (9) $\alpha^{[A]}$ are Lagrange multipliers, $q^{[A]}$ are constant amplitude factors associated with small time-dependent increments in $\alpha^{[A]}$ and the total acoustic tensor $\mathbf{Q}^*$ involves a constitutive part $\mathbf{Q}^c$ together with N reaction components $\mathbf{Q}^{[A]}$ $(A = 1 \ldots N)$ [see e.g. Chadwick *et al.* (1985)]. In addition, the constraint vectors $\mathbf{v}^{[A]}$ are defined by

$$\mathbf{v}^{[A]} = \mathbf{N}^{[A]}\mathbf{n}, \quad (A = 1 \ldots N) \tag{10}$$

in terms of the constraint stress tensors

$$N^{[A]}_{ij} = 2J^{-1} F_{iA} F_{jB} \frac{\partial \lambda^{[A]}}{\partial C_{AB}}, \quad (A = 1 \ldots N). \tag{11}$$

The introduction of the constraint stresses (11) and constraint vectors (10) may be motivated as follows. In the presence of internal constraints upon the deformation gradient the principle of determinism is modified so that the stress $\boldsymbol{\sigma}$ depends upon the deformation gradient $\mathbf{F}$ only to within a stress that does no work in any motion satisfying the constraints.

Since each constraint $\lambda^{[A]}(\mathbf{C}) = 0$ holds for all $\mathbf{X}$ and t, we may take the material time derivative and deduce that

$$\operatorname{tr} \mathbf{N}^{[A]}\mathbf{D} = 0,$$

where $\mathbf{N}^{[A]}$ is defined by eqn (11) and $\mathbf{D}$ is the symmetric part of the spatial velocity gradient. But $\operatorname{tr} \mathbf{N}^{[A]}\mathbf{D}$ is the rate of working of a stress $\mathbf{N}^{[A]}$ and Truesdell and Noll (1965, page 71) have shown that the total stress in a constrained body takes the form

$$\boldsymbol{\sigma}^* = \boldsymbol{\sigma}^c + \sum_{A=1}^{N} \alpha^{[A]}\mathbf{N}^{[A]}, \tag{12}$$

where the constitutive part $\boldsymbol{\sigma}^c$ of the stress is defined by eqn (3). The remainder of the stress arises from the internal forces needed to maintain the constraints but, as we have seen, these do no work in any motion satisfying these constraints. The total stress [eqn (12)] could have been obtained by inserting $\mathbf{W}^*$, defined by eqn (8), into eqn (3) in place of W^c.

The constraint vector $\boldsymbol{\nu}^{[A]}$ defined by eqn (10), corresponding to a general constraint $\lambda^{[A]}(\mathbf{C}) = 0$, was seemingly first introduced, in the context of acceleration wave theory, by Scott (1975) and a full account in the present context of small amplitude plane wave propagation has been given by Chadwick *et al.* (1985). These authors found that the constraints enter into the wave propagation condition (9) only by way of the constraint vectors (10); not all the components of $\mathbf{N}^{[A]}$ are required and the constraint equations themselves, i.e. $\lambda^{[A]}(\mathbf{C}) = 0$, do not appear explicitly.

We note from eqn (9) that the problem is essentially an eigenvalue problem for the quantities v, $\mathbf{e}$ and $q^{[A]}$. Furthermore, in the case of three or more independent constraints ($N \geqslant 3$), the vectors $\boldsymbol{\nu}^{[A]}$ span three-dimensional space for all but certain exceptional directions $\mathbf{n}$ and therefore no solutions of eqn $(9)_2$ exist. The material is then effectively rigid as far as wave propagation is concerned and no waves are able to propagate in non-exceptional directions. In the case $N \leqslant 2$, Chadwick *et al.* (1985) show that in general $3-N$ plane waves propagate in each direction.

The slowness surface now has $3-N$ sheets but more waves may propagate in any exceptional directions resulting in singular behaviour of the slowness surface. It is partly to resolve this anomalous behaviour that the concept of near-constraints is introduced.

2.3. *Nearly constrained materials*

It is possible to relax the mathematical idealization of internal constraints, and to assume that each $\lambda^{[A]}$ is small, and thereby replace the strain energy function (8) by

$$W = W^c + \sum_{A=1}^{N} \tfrac{1}{2}c^{[A]}\{\lambda^{[A]}\}^2, \tag{13}$$

in which $c^{[A]} > 0$ are elastic moduli. In obtaining eqn (13), the strain energy function W has been expanded as a Taylor series about $\lambda^{[A]} = 0$ for each constraint and the linear term omitted. Following Scott (1986) in the case of incompressibility, we omit the linear term since nothing new is gained by its inclusion as is demonstrated later in this subsection. The limit of the exact constraint is realized as $\lambda^{[A]} \to 0$ and $c^{[A]} \to \infty$ in such a way that

$$c^{[A]}\lambda^{[A]} \to \alpha^{[A]}, \quad (A = 1 \ldots N),$$

which remains a bounded quantity. For nearly constrained materials, the product $c^{[A]}\lambda^{[A]}$ plays the same role as does the Lagrange multiplier $\alpha^{[A]}$ in the corresponding constrained material. The expression (12) for the total stress remains valid provided $\alpha^{[A]}$ is interpreted as meaning $c^{[A]}\lambda^{[A]}$. Had linear terms of the form

$$\sum_{A=1}^{N} g^{[A]}\lambda^{[A]},$$

where $g^{[A]}$ is constant, been included in eqn (13), then the only effect on eqn (12) would have been to add $g^{[A]}$ to $\alpha^{[A]}$, a result of no consequence since $\alpha^{[A]}$ is, in any case, arbitrary in the limit of the constraint.

The relevant propagation condition is now the unconstrained condition (6) which, upon employing the strain energy function (13), takes the form

$$\{\rho v^2\mathbf{I}-\mathbf{Q}^*-\sum_{A=1}^{N} Jc^{[A]}\mathbf{v}^{[A]}\otimes\mathbf{v}^{[A]}\}\mathbf{e}=\mathbf{0}, \tag{14}$$

where we have made use of the definition of the constraint vector (10) and where $\mathbf{Q}^*$ is the same as the associated constrained acoustic tensor, apart from $c^{[A]}\lambda^{[A]}$ replacing $\alpha^{[A]}$. It is the quadratic constraint terms in eqn (13) that give rise to the large elastic moduli $c^{[A]}$ occurring in the propagation condition (14). Linear constraint terms make no difference beyond adding $g^{[A]}$ to $\alpha^{[A]}$ as before, and so these linear terms may safely be omitted from eqn (13). If we now identify

$$Jc^{[A]}(\mathbf{v}^{[A]}\cdot\mathbf{e})=\mathrm{q}^{[A]},\quad (A=1\ldots N), \tag{15}$$

the propagation condition (14) may clearly be seen to tend to the constrained condition (9) in the limit. Furthermore, in this limit we must take $c^{[A]}\to\infty$ and $\mathbf{v}^{[A]}\cdot\mathbf{e}\to 0$ in such a way that the product (15) remains bounded; the wave polarization $\mathbf{e}$ is therefore compelled to satisfy eqn $(9)_2$ in the limit. However, it is easily shown that eqn (14) possesses eigenvectors such that $\mathbf{v}^{[A]}\cdot\mathbf{e}\neq 0$ even in the limit when the constraint is operating. We shall see that these correspond to waves of large speed which have no counterpart in the associated constrained problem.

In order to facilitate taking the constrained limit, the dimensionless parameter η is introduced where

$$c^{[A]}=\eta^{-1}\gamma^{[A]},\quad (A=1\ldots N) \tag{16}$$

and $0<\eta\ll 1$. The scaled elastic moduli $\gamma^{[A]}$ are independent of η and comparable in magnitude to a typical component of the constitutive elastic modulus $\mathbf{d}^c$. The constraint limits $c^{[A]}\to\infty$ then correspond to $\eta\to 0$ with $\gamma^{[A]}$ remaining fixed. The acoustic tensor may now be written as

$$\mathbf{Q}=\mathbf{Q}^*+\eta^{-1}\mathbf{M},\quad \mathbf{M}=\sum_{A=1}^{N} J\gamma^{[A]}\mathbf{v}^{[A]}\otimes\mathbf{v}^{[A]}, \tag{17}$$

in which the non-zero components of $\mathbf{Q}^*$ and $\mathbf{M}$ are of comparable magnitude (unless the direction of wave propagation is such that all of the N associated constraint vectors vanish).

Since a nearly constrained material is, in fact, unconstrained it possesses a three-sheeted slowness surface. As the constraint limit is approached this slowness surface tends to become singular and resemble that of the constrained material. Taking this limit is discussed and graphically illustrated in Section 6.

3. TWO EXACT CONSTRAINTS

We shall now consider the problem of wave propagation in elastic solids subject to two exact internal constraints. As was indicated in the previous section, this is the maximum

number which may be imposed before wave propagation becomes possible only in exceptional directions. From eqn (9) the propagation condition associated with this doubly constrained problem may be written explicitly in the form

$$(\rho v^2\mathbf{I}-\mathbf{Q}^*)\mathbf{e}-q^{[1]}\mathbf{v}^{[1]}-q^{[2]}\mathbf{v}^{[2]}=\mathbf{0}, \quad \mathbf{v}^{[1]}\cdot\mathbf{e}=\mathbf{v}^{[2]}\cdot\mathbf{e}=0. \tag{18}$$

3.1. *Non-exceptional directions*

It is readily deduced that a single wave is able to propagate in any non-exceptional direction. The unit polarization vector and wave speed associated with this wave are given by

$$\mathbf{e}=\frac{\mathbf{v}^{[1]}\wedge\mathbf{v}^{[2]}}{|\mathbf{v}^{[1]}\wedge\mathbf{v}^{[2]}|}\overset{\text{def}}{=}\hat{\mathbf{u}}, \quad \rho v^2=\hat{\mathbf{u}}\cdot(\mathbf{Q}^*\hat{\mathbf{u}}). \tag{19}$$

Furthermore, this wave will be a homogeneous wave, i.e. having a real wave speed, provided that

$$\hat{\mathbf{u}}\cdot(\mathbf{Q}^c\hat{\mathbf{u}})+\alpha^{[1]}\hat{\mathbf{u}}\cdot(\mathbf{Q}^{[1]}\hat{\mathbf{u}})+\alpha^{[2]}\hat{\mathbf{u}}\cdot(\mathbf{Q}^{[2]}\hat{\mathbf{u}})>0. \tag{20}$$

A physically realistic response for unconstrained solids may be ensured by imposing the strong ellipticity condition on $\mathbf{d}^c$, in which case the first term on the left-hand side of eqn (20) may certainly be assumed positive. It is observed however, that even if both $\mathbf{Q}^{[1]}$ and $\mathbf{Q}^{[2]}$ satisfy such a condition (as is the case for most commonly encountered constraints), the two Lagrange multipliers $\alpha^{[1]}$ and $\alpha^{[2]}$ may always be chosen sufficiently negative to ensure that eqn (20) is violated. For any specific constraint the Lagrange multiplier may be physically interpreted, e.g. as an arbitrary tension along the fibre direction in the case of inextensibility. It was first noted by Chen and Gurtin (1972), that, in the context of inextensibility, a compressive tension along the fibres of a large enough magnitude results in a purely imaginary wave speed. Such a wave speed leads to growing exponential terms which were thought to imply a loss of stability in some sense. However, a recent paper (Fu, 1993) has shown that the inclusion of non-linear terms in the governing equations leads to a stabilization of the motion. In those cases where the large exponential terms occur, it would appear that the assumptions of linear elasticity are violated and we therefore restrict attention purely to the case in which the inequality (20) holds.

3.2. *Exceptional directions*

It has already been noted that in a doubly constrained elastic solid only a single plane wave is able to propagate in each non-exceptional direction. In this section the propagation of waves in the three distinct classes of exceptional direction is discussed.

Case (i) $\mathbf{v}^{[1]}\neq\mathbf{0}$, $\mathbf{v}^{[2]}=\mathbf{0}$. In the case $\mathbf{v}^{[1]}\neq\mathbf{0}$, $\mathbf{v}^{[2]}=\mathbf{0}$, the propagation condition (18) may be cast into the form

$$(\rho v^2\mathbf{I}-\mathbf{P}\mathbf{Q}^*)\mathbf{e}=\mathbf{0}, \quad \mathbf{P}=\mathbf{I}-\hat{\mathbf{v}}^{[1]}\otimes\hat{\mathbf{v}}^{[1]}, \quad \mathbf{e}\cdot\hat{\mathbf{v}}^{[1]}=0, \tag{21}$$

where eqn $(18)_3$ now places no restriction upon $\mathbf{e}$ and $\hat{\mathbf{v}}^{[1]}$ denotes a unit vector parallel to $\mathbf{v}^{[1]}$. The propagation condition (21) has the same general form as that corresponding to wave propagation in a singly constrained elastic solid [see Rogerson and Scott (1992a), eqns (3.10), (3.11)]. The only difference between the present eqn (21) and the propagation condition of the corresponding singly constrained problem is the subtle one of the possible occurrence in $\mathbf{Q}^*$ of terms associated with the inactive constraint. The conclusion in this case is that *two* plane waves may propagate with wave speeds and polarizations satisfying eqn (21).

Case (ii) $\mathbf{v}^{[1]} = \mathbf{0}$, $\mathbf{v}^{[2]} = \mathbf{0}$. In the exceptional directions for which both constraint vectors vanish, the propagation condition takes the form of the unconstrained condition (6). Again there is a possibility that terms associated with the inactive constraints still make a non-zero contribution to the acoustic tensor. If this is the case it is certainly *not* possible to conclude that three homogeneous waves may propagate, even if the constitutive part $\mathbf{Q}^c$ of $\mathbf{Q}^*$ satisfies the strong ellipticity condition. Nevertheless, for appropriate values of the scalars $\alpha^{[1]}$ and $\alpha^{[2]}$, we may conclude that in these exceptional directions three homogeneous plane waves may propagate.

Case (iii) $\alpha\mathbf{v}^{[1]} + \beta\mathbf{v}^{[2]} = \mathbf{0}$. In the case in which the two constraint vectors are parallel with neither vanishing, the propagation condition takes the form

$$(\rho v^2\mathbf{I} - \mathbf{Q}^*)\mathbf{e} - (q^{[1]} - (\alpha/\beta)q^{[2]})\hat{\mathbf{v}}^{[1]} = \mathbf{0}, \quad \hat{\mathbf{v}}^{[1]} \cdot \mathbf{e} = 0. \tag{22}$$

This is the form of the singly constrained condition which may be cast into a form equivalent to eqn (21), indicating that two plane waves may propagate in such directions.

4. TWO NEAR-CONSTRAINTS

In this section the general theory outlined in Section 2.3 is applied to the particular case of two near-constraints. This is of particular interest as it is the maximum number of constraints for which wave propagation is possible in every direction. Upon invoking a combination of eqns (14), (16) and (17), the appropriate propagation condition is expressible in the form

$$(\lambda\mathbf{I} - \mathbf{Q}^* - \eta^{-1}\mathbf{M})\mathbf{e} = \mathbf{0}, \quad \mathbf{M} = J(\gamma^{[1]}\mathbf{v}^{[1]} \otimes \mathbf{v}^{[1]} + \gamma^{[2]}\mathbf{v}^{[2]} \otimes \mathbf{v}^{[2]}), \tag{23}$$

in which, for convenience, ρv^2 has been replaced by λ. It is tacitly assumed here that the propagation direction is neither in, nor close to, any exceptional direction. Series solutions of the propagation condition are now sought in the form

$$\lambda = \eta^{-1}\lambda_{-1} + \lambda_0 + \eta\lambda_1 + \mathrm{O}(\eta^2), \quad \mathbf{e} = \mathbf{e}_0 + \eta\mathbf{e}_1 + \eta^2\mathbf{e}_2 + \mathrm{O}(\eta^3), \tag{24}$$

which, when inserted into eqns (23), yield the three leading-order equations

$$\lambda_1\mathbf{e}_{i-2} + (\lambda_0\mathbf{I} - \mathbf{Q}^*)\mathbf{e}_{i-1} + (\lambda_{-1}\mathbf{I} - \mathbf{M})\mathbf{e}_i = \mathbf{0}, \quad (i = 0, 1, 2), \tag{25}$$

in which we take $\mathbf{e}_j = 0$ if the subscript j is negative.

At this stage our discussion is restricted to non-exceptional directions so that $\mathbf{M}$ has rank 2 and may consequently be written as

$$\mathbf{M} = \mu_2\mathbf{m}_2 \otimes \mathbf{m}_2 + \mu_3\mathbf{m}_3 \otimes \mathbf{m}_3, \tag{26}$$

where $\mathbf{m}_2$ and $\mathbf{m}_3$ are the two orthogonal unit eigenvectors of $\mathbf{M}$ with associated non-zero eigenvalues μ_2 and μ_3. The leading-order equation is obtained from eqn (25) by putting $i = 0$. From this equation it is clear that there are two distinct cases.

Case (i) $\lambda_{-1} = 0$. In the case $\lambda_{-1} = 0$, the associated leading-order eigenvector is given by

$$\mathbf{e}_0^{(1)} = \frac{\mathbf{v}^{[1]} \wedge \mathbf{v}^{[2]}}{|\mathbf{v}^{[1]} \wedge \mathbf{v}^{[2]}|} \equiv \mathbf{m}_1. \tag{27}$$

The second- and third-order equations may now be obtained from eqn (23) by setting $i = 1, 2$ and the following series expansions obtained:

$$\lambda^{(1)} = \mathbf{m}_1 \cdot (\mathbf{Q}^* \mathbf{m}_1) - \eta \left\{ \frac{[\mathbf{m}_2 \cdot (\mathbf{Q}^* \mathbf{m}_1)]^2}{\mu_2} + \frac{[\mathbf{m}_3 \cdot (\mathbf{Q}^* \mathbf{m}_1)]^2}{\mu_3} \right\} + O(\eta^2) \tag{28}$$

$$\mathbf{e}^{(1)} = \mathbf{m}_1 - \eta \left\{ \frac{1}{\mu_2} \mathbf{m}_2 \otimes \mathbf{m}_2 + \frac{1}{\mu_3} \mathbf{m}_3 \otimes \mathbf{m}_3 \right\} \mathbf{Q}^* \mathbf{m}_1 + O(\eta^2). \tag{29}$$

In obtaining the two expansions (28) and (29), use has been made of the fact that $\mathbf{e}$ is a unit vector from which it follows that $\mathbf{e}_0 \cdot \mathbf{e}_0 = 1$ and $\mathbf{e}_0 \cdot \mathbf{e}_1 = 0$.

Case (ii) $\lambda_{-1} \neq 0$. In this case our concern is the two waves which in general fail to retain finite wave speed in the limit $\eta \to 0$; these two waves have no counterpart in the doubly constrained theory. The leading-order eigenvalues and eigenvectors are those associated with the two non-zero eigenvalues of $\mathbf{M}$ and are denoted by

$$\lambda_{-1}^{(2)} = \mu_2, \quad \mathbf{e}_0^{(2)} = \mathbf{m}_2, \quad \lambda_{-1}^{(3)} = \mu_3, \quad \mathbf{e}_0^{(3)} = \mathbf{m}_3. \tag{30}$$

It is now possible to represent both second-order eqns (25), each associated with one of the two propagating waves, in the forms

$$(\lambda_0^{(2)} \mathbf{I} - \mathbf{Q}^*) \mathbf{m}_2 + \{\mu_2 \mathbf{m}_1 \otimes \mathbf{m}_1 + (\mu_2 - \mu_3) \mathbf{m}_3 \otimes \mathbf{m}_3\} \mathbf{e}_1^{(2)} = \mathbf{0} \tag{31}$$

$$(\lambda_0^{(3)} \mathbf{I} - \mathbf{Q}^*) \mathbf{m}_3 + \{\mu_3 \mathbf{m}_1 \otimes \mathbf{m}_1 + (\mu_3 - \mu_2) \mathbf{m}_2 \otimes \mathbf{m}_2\} \mathbf{e}_1^{(3)} = \mathbf{0}, \tag{32}$$

which are obtained by representing both $\mathbf{I}$ and $\mathbf{M}$ in spectral form.

The fact that $\mathbf{m}_\alpha \cdot \mathbf{e}_1^{(\alpha)} = 0$ ($\alpha = 2, 3$) is now used to deduce that

$$\lambda_0^{(\alpha)} = \mathbf{m}_\alpha \cdot (\mathbf{Q}^* \mathbf{m}_\alpha), \quad (\alpha = 2, 3). \tag{33}$$

In addition, it is clear that $\mathbf{e}_1^{(2)}$ is a linear combination of $\mathbf{m}_1$ and $\mathbf{m}_3$, whilst $\mathbf{e}_1^{(3)}$ is a linear combination of $\mathbf{m}_1$ and $\mathbf{m}_2$. Using eqns (31) and (32) we may deduce expressions for $\mathbf{e}_1^{(2)}$ and $\mathbf{e}_1^{(3)}$ and then insert both them and eqn (30) into eqn (24) to obtain

$$\mathbf{e}^{(2)} = \mathbf{m}_2 + \eta \left\{ \frac{1}{\mu_2} \mathbf{m}_1 \otimes \mathbf{m}_1 + \frac{1}{\mu_2 - \mu_3} \mathbf{m}_3 \otimes \mathbf{m}_3 \right\} \mathbf{Q}^* \mathbf{m}_2 + O(\eta^2) \tag{34}$$

$$\mathbf{e}^{(3)} = \mathbf{m}_3 + \eta \left\{ \frac{1}{\mu_3} \mathbf{m}_1 \otimes \mathbf{m}_1 + \frac{1}{\mu_3 - \mu_2} \mathbf{m}_2 \otimes \mathbf{m}_2 \right\} \mathbf{Q}^* \mathbf{m}_3 + O(\eta^2). \tag{35}$$

The third-order eqn $(25)_3$ may now be used to determine expressions for $\lambda_1^{(\alpha)}$ ($\alpha = 2, 3$) and yields

$$\lambda^{(2)} = \frac{\mu_2}{\eta} + \mathbf{m}_2 \cdot (\mathbf{Q}^* \mathbf{m}_2) + \eta \left\{ \frac{[\mathbf{m}_1 \cdot (\mathbf{Q}^* \mathbf{m}_2)]^2}{\mu_2} + \frac{[\mathbf{m}_3 \cdot (\mathbf{Q}^* \mathbf{m}_2)]^2}{\mu_2 - \mu_3} \right\} + O(\eta^2) \tag{36}$$

$$\lambda^{(3)} = \frac{\mu_3}{\eta} + \mathbf{m}_3 \cdot (\mathbf{Q}^* \mathbf{m}_3) + \eta \left\{ \frac{[\mathbf{m}_1 \cdot (\mathbf{Q}^* \mathbf{m}_3)]^2}{\mu_3} + \frac{[\mathbf{m}_2 \cdot (\mathbf{Q}^* \mathbf{m}_3)]^2}{\mu_3 - \mu_2} \right\} + O(\eta^2). \tag{37}$$

The eigenvalues and corresponding eigenvector expansions which have been obtained in this section may be summarized as follows:

$$\lambda^{(\alpha)} = \frac{\mu_\alpha}{\eta} + \mathbf{m}_\alpha \cdot (\mathbf{Q}^*\mathbf{m}_\alpha) + \eta \sum_{\beta=1}^{3}{}' \frac{[\mathbf{m}_\beta \cdot (\mathbf{Q}^*\mathbf{m}_\alpha)]^2}{\mu_\alpha - \mu_\beta} + O(\eta^2) \tag{38}$$

$$\mathbf{e}^{(\alpha)} = \mathbf{m}_\alpha + \eta \left(\sum_{\beta=1}^{3}{}' \frac{\mathbf{m}_\beta \otimes \mathbf{m}_\beta}{\mu_\alpha - \mu_\beta} \right) \mathbf{Q}^*\mathbf{m}_\alpha + O(\eta^2), \tag{39}$$

for $\alpha = 1, 2, 3$. In eqns (38) and (39) we must take $\mu_1 = 0$ and omit the $\beta = \alpha$ term from each summation, as indicated by the prime.

It is of interest to note that to within $O(\eta^2)$, the orthonormal set $\{\mathbf{e}^{(1)}, \mathbf{e}^{(2)}, \mathbf{e}^{(3)}\}$ is a rotation of the orthonormal set $\{\mathbf{m}_1, \mathbf{m}_2, \mathbf{m}_3\}$. It is therefore deduced that to within $O(\eta^2)$,

$$\mathbf{e}^{(\alpha)} = \mathbf{R}\mathbf{m}_\alpha, \quad (\alpha = 1, 2, 3) \quad \text{where} \quad R_{ij} = \delta_{ij} + \eta \varepsilon_{ijk} \chi_k \tag{40}$$

and ε_{ijk} denotes the permutation symbol. The quantities R_{ij} are the components of a rotation tensor $\mathbf{R}$ and the quantities χ_k are the components of a vector with respect to the orthonormal set $\{\mathbf{m}_1, \mathbf{m}_2, \mathbf{m}_3\}$ given explicitly by

$$\chi_k = \varepsilon_{kpq} \frac{\mathbf{m}_p \cdot (\mathbf{Q}^*\mathbf{m}_q)}{\mu_p - \mu_q},$$

where the subscripts p and q are summed over, omitting those terms with $p = q$, and again we take $\mu_1 = 0$. More explicitly in direct notation we have

$$\boldsymbol{\chi} = \frac{[\mathbf{m}_2 \cdot (\mathbf{Q}^*\mathbf{m}_3)]\mathbf{m}_1}{\mu_2 - \mu_3} + \frac{[\mathbf{m}_3 \cdot (\mathbf{Q}^*\mathbf{m}_1)]\mathbf{m}_2}{\mu_3} - \frac{[\mathbf{m}_1 \cdot (\mathbf{Q}^*\mathbf{m}_2)]\mathbf{m}_3}{\mu_2}.$$

The direction of the vector $\boldsymbol{\chi}$ gives the axis of rotation of $\mathbf{R}$ and $-\eta|\boldsymbol{\chi}|$ is the angle of rotation, which is small with η.

5. WAVE PROPAGATION IN THE NEIGHBOURHOOD OF AN EXCEPTIONAL DIRECTION

We now investigate wave propagation in the neighbourhood of exceptional directions, i.e. directions in which the two constraint vectors $\boldsymbol{v}^{[1]}$ and $\boldsymbol{v}^{[2]}$ fail to be linearly independent. To begin we recall from eqn (24) and (30) that the two non-zero leading-order squared wave speeds are given by μ_2/η and μ_3/η, where μ_2 and μ_3 are the two roots of the quadratic equation

$$\mu^2 - (\text{tr } \mathbf{M})\mu + \tfrac{1}{2}\{(\text{tr } \mathbf{M})^2 + \text{tr } (\mathbf{M}^2)\} = 0. \tag{41}$$

Upon invoking the definition of $\mathbf{M}$ given in eqn $(17)_2$, it is possible to deduce that

$$\text{tr } \mathbf{M} = J \sum_{A=1}^{2} \gamma^{[A]} \boldsymbol{v}^{[A]} \cdot \boldsymbol{v}^{[A]} \tag{42}$$

$$\text{tr } (\mathbf{M}^2) = J^2 \sum_{A=1}^{2} \sum_{B=1}^{2} \gamma^{[A]} \gamma^{[B]} (\boldsymbol{v}^{[A]} \cdot \boldsymbol{v}^{[B]})^2. \tag{43}$$

After a little algebraic manipulation it is possible to represent the two roots of eqn (41) in the explicit forms

$$\mu_{2,3} = \frac{J}{2}\{\gamma^{[1]}\boldsymbol{v}^{[1]}\cdot\boldsymbol{v}^{[1]} + \gamma^{[2]}\boldsymbol{v}^{[2]}\cdot\boldsymbol{v}^{[2]}\} \pm \frac{J}{2}\{(\gamma^{[1]}\boldsymbol{v}^{[1]}\cdot\boldsymbol{v}^{[1]} + \gamma^{[2]}\boldsymbol{v}^{[2]}\cdot\boldsymbol{v}^{[2]})^2 - 4\gamma^{[1]}\gamma^{[2]}|\boldsymbol{v}^{[1]}\wedge\boldsymbol{v}^{[2]}|^2\}^{1/2}$$

(44)

$$\mu_{2,3} = \frac{J}{2}\{\gamma^{[1]}\boldsymbol{v}^{[1]}\cdot\boldsymbol{v}^{[1]} + \gamma^{[2]}\boldsymbol{v}^{[2]}\cdot\boldsymbol{v}^{[2]}\} \pm \frac{J}{2}\{(\gamma^{[1]}\boldsymbol{v}^{[1]}\cdot\boldsymbol{v}^{[1]} - \gamma^{[2]}\boldsymbol{v}^{[2]}\cdot\boldsymbol{v}^{[2]})^2 + 4\gamma^{[1]}\gamma^{[2]}(\boldsymbol{v}^{[1]}\cdot\boldsymbol{v}^{[2]})^2\}^{1/2}.$$

From eqn $(44)_2$ we see that both μ_2 and μ_3 are real and from eqn $(44)_1$ that both are positive since $\gamma^{[1]}$ and $\gamma^{[2]}$ are positive.

Case (i) $\boldsymbol{v}^{[2]}\cdot\boldsymbol{v}^{[2]}$ *is small and* $\boldsymbol{v}^{[1]}\cdot\boldsymbol{v}^{[1]}$ *is* O(1). In this section the propagation of waves in the neighbourhood of directions in which $\boldsymbol{v}^{[2]}$ vanishes but $\boldsymbol{v}^{[1]}$ does not is discussed. Upon the assumption that $\boldsymbol{v}^{[2]}\cdot\boldsymbol{v}^{[2]}$ is small the two solutions of eqn (44) may be expanded to yield

$$\mu_2 = \frac{J\gamma^{[1]}\boldsymbol{v}^{[1]}\cdot\boldsymbol{v}^{[1]}}{2} + \frac{J\gamma^{[2]}(\boldsymbol{v}^{[1]}\cdot\boldsymbol{v}^{[2]})^2}{2\boldsymbol{v}^{[1]}\cdot\boldsymbol{v}^{[1]}} + O(\boldsymbol{v}^{[2]}\cdot\boldsymbol{v}^{[2]})^2 \tag{45}$$

and

$$\mu_3 = \frac{J\gamma^{[2]}\boldsymbol{v}^{[2]}\cdot\boldsymbol{v}^{[2]}}{2} - \frac{J\gamma^{[2]}(\boldsymbol{v}^{[1]}\cdot\boldsymbol{v}^{[2]})^2}{2\boldsymbol{v}^{[1]}\cdot\boldsymbol{v}^{[1]}} + O(\boldsymbol{v}^{[2]}\cdot\boldsymbol{v}^{[2]})^2. \tag{46}$$

It is clear from eqn (45) that as $\boldsymbol{v}^{[2]}\cdot\boldsymbol{v}^{[2]} \to 0$, the leading-order term retains finite value implying that the corresponding squared wave speed μ_2/η remains large and tends to infinity as the constrained limits $\eta \to 0$ is reached. In contrast, the second approximate solution μ_3, given by eqn (46), clearly tends to zero as $\boldsymbol{v}^{[2]}\cdot\boldsymbol{v}^{[2]} \to 0$ so that the associated squared wave speed remains finite even in the constrained limit. The interpretation of this result is that one of the squared wave speeds, specifically the one associated with eqn (46), changes rapidly from $O(\eta^{-1})$ to O(1) in the neighbourhood of such exceptional directions. The regions within which such changes occur are characterized by

$$\eta^{-1}(\boldsymbol{v}^{[2]}\cdot\boldsymbol{v}^{[2]}) \equiv m = O(1). \tag{47}$$

In such regions it is clear from eqns (38) and (39) that the expansion solutions for the eigenvalues and eigenvectors are no longer valid as rapid changes occur to both solutions in this case even as $\boldsymbol{v}^{[2]}\cdot\boldsymbol{v}^{[2]} \to 0$. It is of interest to note that these changes also occur to the wave speed associated with the single wave which is able to propagate in a doubly constrained solid. The implication is that this wave speed is discontinuous in the exceptional direction. A fuller discussion of this interesting phenomenon can be found in recent papers by Rogerson and Scott (1993) and Scott (1992b) in the context of a single constraint. The conclusion is that two of the wave speeds retain finite magnitude in the constrained limit; this is consistent with the finite speed of the two waves observed to propagate in a similar direction in the doubly constrained solid discussed in Section 3.2.

Case (ii) $\boldsymbol{v}^{[1]}\cdot\boldsymbol{v}^{[1]}$ *and* $\boldsymbol{v}^{[2]}\cdot\boldsymbol{v}^{[2]}$ *both small.* In the neighbourhood of directions in which both constraint vectors vanish, all the terms on the right-hand side of eqn (44) are small. Furthermore, when the direction of propagation actually lies in a direction such that $\boldsymbol{v}^{[1]} = \boldsymbol{0}$ and $\boldsymbol{v}^{[2]} = \boldsymbol{0}$ then the right-hand side of eqn (44) is zero. It may be concluded that in the neighbourhood of such directions both values of μ are small. This indicates that the two corresponding leading-order solutions obtained from eqn (38) are O(1) close to such exceptional directions. For wave propagation either in, or close to, these directions all three wave speeds are therefore O(1) and remain O(1) even in the constrained limit. In Section 3.2 it was seen that such a direction in a doubly constrained solid afforded the full complement of three propagating waves.

Case (iii) $\mathbf{v}^{[1]}$ *and* $\mathbf{v}^{[2]}$ *parallel or almost parallel.* In order to elucidate the propagation of waves close to directions $\mathbf{n}$ for which the two constraint vectors are parallel, we introduce ψ as the angle between them and accordingly assume that ψ is small. It is now possible to represent eqn (44) in the form

$$\mu_{2,3} = \frac{J}{2}\{\gamma^{[1]}\mathbf{v}^{[1]}\cdot\mathbf{v}^{[1]} + \gamma^{[2]}\mathbf{v}^{[2]}\cdot\mathbf{v}^{[2]}\} \pm \frac{J}{2}\{(\gamma^{[1]}\mathbf{v}^{[1]}\cdot\mathbf{v}^{[1]} + \gamma^{[2]}\mathbf{v}^{[2]}\cdot\mathbf{v}^{[2]})^2 - 4\gamma^{[1]}\gamma^{[2]}(\mathbf{v}^{[1]}\cdot\mathbf{v}^{[1]})(\mathbf{v}^{[2]}\cdot\mathbf{v}^{[2]})\sin^2\psi\}^{1/2}. \quad (48)$$

After a little manipulation we obtain the approximate solutions

$$\mu_2 = \frac{J}{2}\{\gamma^{[1]}\mathbf{v}^{[1]}\cdot\mathbf{v}^{[1]} + \gamma^{[2]}\mathbf{v}^{[2]}\cdot\mathbf{v}^{[2]}\} - \frac{J\gamma^{[1]}\gamma^{[2]}(\mathbf{v}^{[1]}\cdot\mathbf{v}^{[1]})(\mathbf{v}^{[2]}\cdot\mathbf{v}^{[2]})\sin^2\psi}{2\{\gamma^{[1]}\mathbf{v}^{[1]}\cdot\mathbf{v}^{[1]} + \gamma^{[2]}\mathbf{v}^{[2]}\cdot\mathbf{v}^{[2]}\}} + O(\sin^4\psi) \quad (49)$$

$$\mu_3 = \frac{J\gamma^{[1]}\gamma^{[2]}(\mathbf{v}^{[1]}\cdot\mathbf{v}^{[1]})(\mathbf{v}^{[2]}\cdot\mathbf{v}^{[2]})\sin^2\psi}{2\{\gamma^{[1]}\mathbf{v}^{[1]}\cdot\mathbf{v}^{[1]} + \gamma^{[2]}\mathbf{v}^{[2]}\cdot\mathbf{v}^{[2]}\}} + O(\sin^4\psi). \quad (50)$$

Since $\sin\psi$ is small with ψ, only the solution given by eqn (49) remains finite as $\psi \to 0$ which implies that the corresponding wave speed is large and tends to infinity in the constrained limit. In contrast, the solution given by eqn (50) tends to zero as $\psi \to 0$ and the corresponding wave speed remains finite even in the constrained limit. The conclusion is that there is a region around such exceptional directions characterized by $\eta^{-1}\sin^2\psi = O(1)$ in which one of the two large wave speeds rapidly reduces in magnitude to O(1). These deductions elucidate the observations made in Section 3.2 for the corresponding doubly constrained case.

6. ILLUSTRATIVE EXAMPLES AND CROSS-SECTIONS OF THE SLOWNESS SURFACE

The theory presented in the previous sections will now be illustrated by means of two examples concerning doubly constrained elastic solids. Both of these examples involve the constraints of incompressibility and inextensibility. These are by no means the only constraints of importance in solid mechanics but are the two most commonly encountered. We shall begin with a brief review of the salient features of the two constraints.

Incompressibility

All motions of an incompressible elastic body are necessarily isochoric and it follows that the constraint function may be taken in the form

$$\lambda^{[1]}(\mathbf{C}) \equiv (\det\mathbf{C})^{1/2} - 1 = 0 \quad (51)$$

[see Chadwick (1976)]. From this constraint function it is possible to deduce that

$$N_{ij}^{[1]} = \delta_{ij}, \quad v_i^{[1]} = n_i, \quad d_{ijkl}^{[1]} = \delta_{ij}\delta_{kl} - \delta_{il}\delta_{jk}, \quad Q_{ik}^{[1]} = 0. \quad (52)$$

The corresponding Lagrange multiplier is now interpreted as the negative of an arbitrary pressure needed to maintain the constraint of incompressibility. We note, however, that in view of eqn $(52)_4$ this multiplier does not appear in the corresponding total acoustic tensor. This would appear to be a phenomenon peculiar to the constraint of incompressibility. The constraint vector $(52)_2$ is non-zero for every direction of propagation and so there are no exceptional directions.

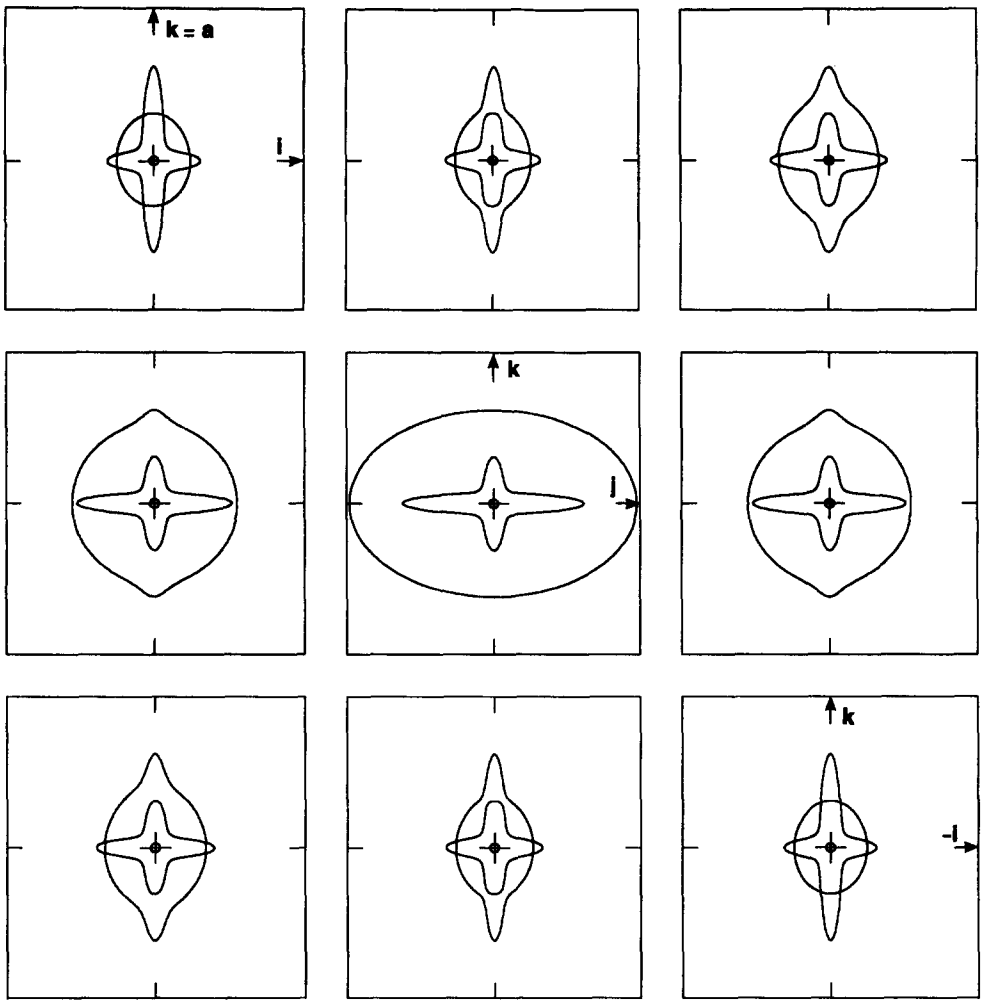

Fig. 1. Cross-sections of the slowness surface of a virtually incompressible, nearly inextensible elastic material: $c_1 = 1$, $c_2 = 1$, $\kappa = 1000$, $E = 200$; $\lambda_1 = 2$, $\lambda_2 = \frac{1}{2}$, $\lambda_3 = 1$.

Inextensibility

The constraint of inextensibility along a family of parallel material lines has been used in the last few years as an ingredient of models describing the mechanical properties of fibre-reinforced materials in which the fibres are taken to be inextensible. For this reason we shall often refer to the direction of inextensibility as the fibre direction. An appropriate constraint function may be taken to be

$$\lambda^{[2]}(\mathbf{C}) \equiv \tfrac{1}{2}\{\mathbf{A}\cdot(\mathbf{CA}) - 1\} = 0, \tag{53}$$

where $\mathbf{A}$ is a unit vector parallel to the fibre direction in B_u [see e.g. Spencer (1972)]. This constraint function may be used to deduce that

$$N_{ij}^{[2]} = J^{-1}a_i a_j, \quad v_i^{[2]} = J^{-1}(\mathbf{a}\cdot\mathbf{n})a_i, \quad d_{ijkl}^{[2]} = J^{-1}\delta_{ik}a_j a_l, \quad Q_{ik}^{[2]} = J^{-1}(\mathbf{a}\cdot\mathbf{n})^2\delta_{ik}, \tag{54}$$

in which $\mathbf{a} = \mathbf{FA}$ gives the orientation of the fibres in B_e. For this constraint the arbitrary Lagrange multiplier may be interpreted as a tension along the fibre direction. From eqn $(54)_2$ it is noted that the constraint vector vanishes when $\mathbf{a}\cdot\mathbf{n} = 0$, i.e. when the direction of wave propagation is normal to the fibre orientation in B_e. Thus there is a whole plane of exceptional directions of wave propagation, namely, the plane with normal parallel to the

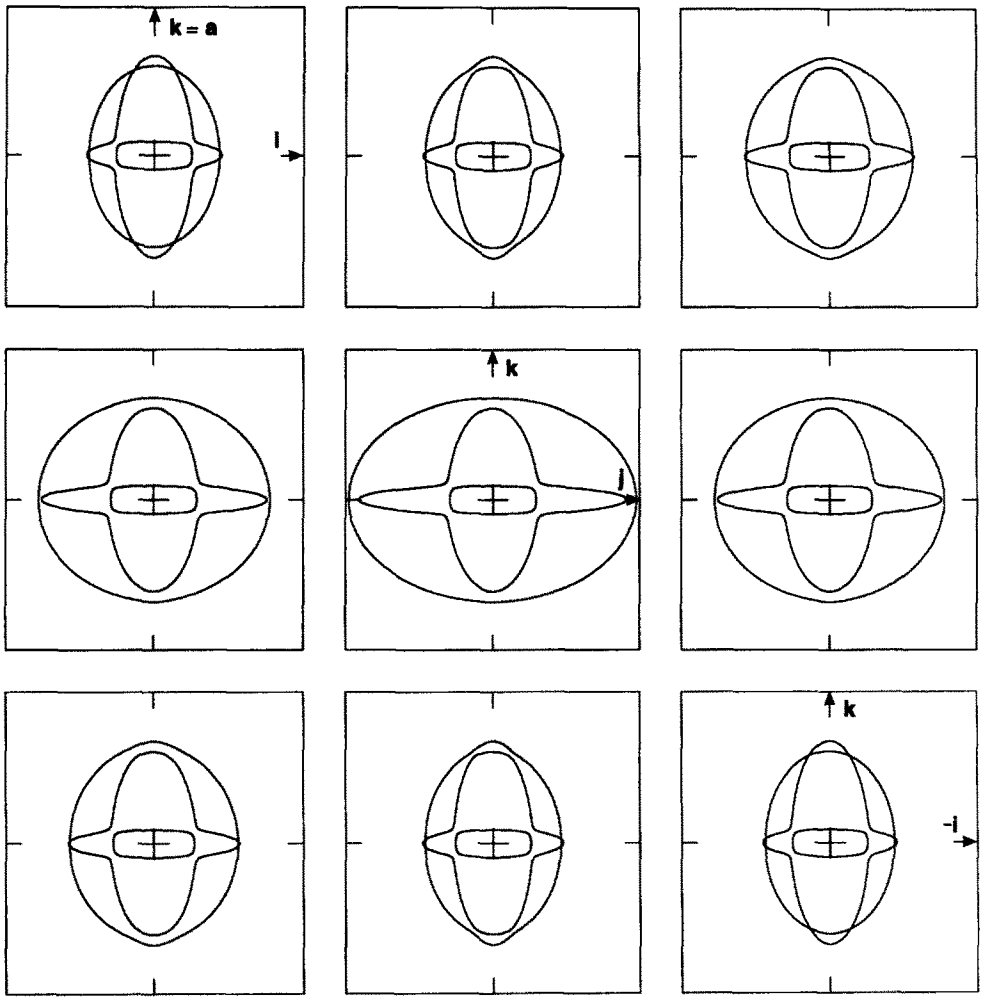

Fig. 2(a). Cross-sections of the slowness surface of a fairly incompressible, nearly inextensible elastic material: $c_1 = 1$, $c_2 = 0.14$, $\kappa = 10$, $E = 100$; $\lambda_1 = \frac{3}{2}$, $\lambda_2 = \frac{2}{3}$, $\lambda_3 = 1$.

fibre direction. Wave propagation in an inextensible material was first discussed by Chen and Gurtin (1972).

6.1. *Incompressibility and inextensibility*

The specific results quoted for incompressibility and inextensibility may now be used in conjunction with eqn (18) to establish the appropriate propagation condition for a material that is both incompressible and inextensible in the direction $\mathbf{a}$:

$$\{[\rho v^2 - T(\mathbf{a}\cdot\mathbf{n})^2]\mathbf{I} - \mathbf{Q}^c\}\mathbf{e} + T^*(\mathbf{a}\cdot\mathbf{n})\mathbf{a} - p^*\mathbf{n} = \mathbf{0} \tag{55}$$

$$\mathbf{n}\cdot\mathbf{e} = 0, \quad (\mathbf{a}\cdot\mathbf{n})(\mathbf{a}\cdot\mathbf{e}) = 0, \tag{56}$$

in which T is an arbitrary tension in B_e and T^* and p^* are the amplitudes of the small time-dependent perturbations of the Lagrange multipliers from their equilibrium states.

We may deduce that a single wave propagates in each non-exceptional direction by means of analysis closely paralleling that of the general case discussed in Section 3.1. In the first exceptional case, in which $\mathbf{a}\cdot\mathbf{n} = 0$, it is possible to cast the propagation conditions into the form

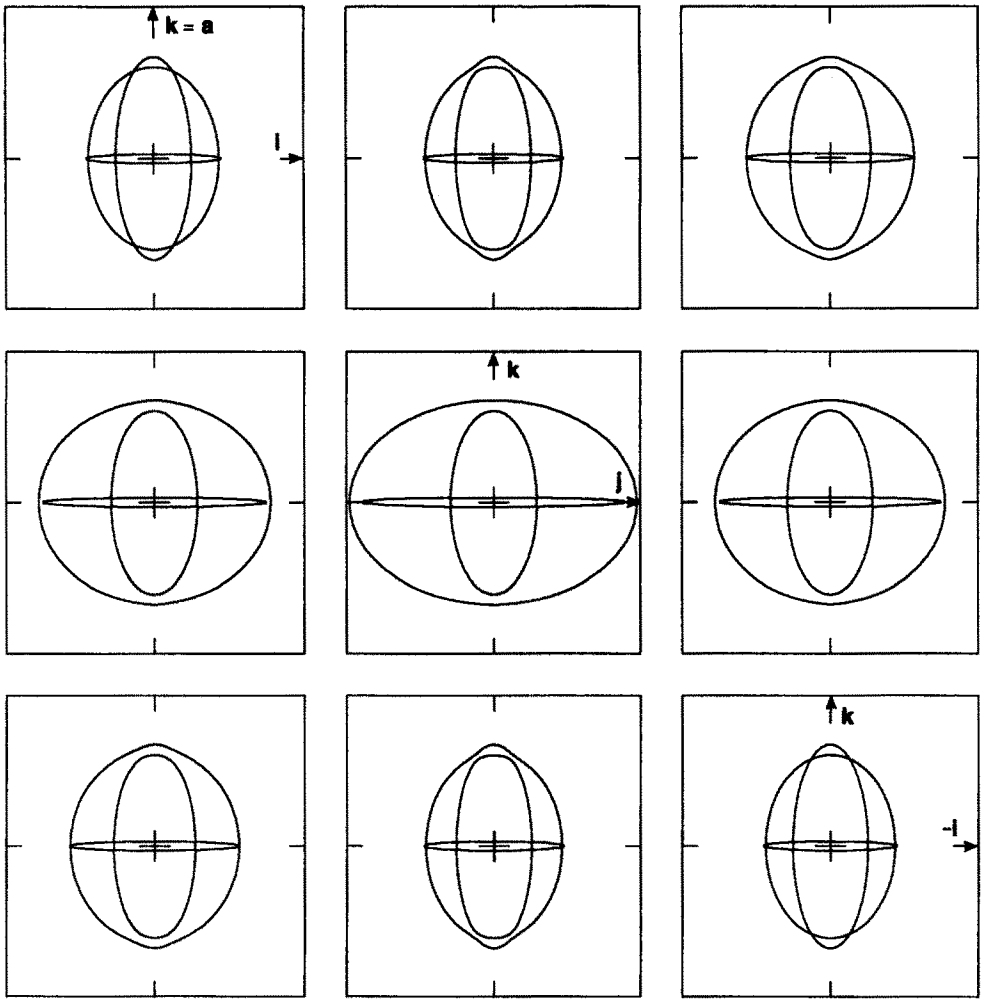

Fig. 2(b). Cross-sections of the slowness surface of a fairly incompressible, virtually inextensible elastic material: $c_1 = 1$, $c_2 = 0.14$, $\kappa = 10$, $E = 1000$; $\lambda_1 = \frac{3}{2}$, $\lambda_2 = \frac{2}{3}$, $\lambda_3 = 1$.

$$(\rho v^2 \mathbf{I} - \mathbf{P}\mathbf{Q}^c)\mathbf{e} = \mathbf{0}, \quad \mathbf{P} = \mathbf{I} - \mathbf{n} \otimes \mathbf{n}, \tag{57}$$

and eqn $(56)_2$ is now satisfied without any further restriction on $\mathbf{e}$. Equation (57) is the propagation condition appropriate to the single constraint of incompressibility and furnishes two plane waves [see e.g. Scott (1986)]. For the second type of exceptional case which occurs, when the direction of propagation is along the fibres so that $\mathbf{n} = \pm\mathbf{a}$, eqn (55) takes the form

$$\{[\rho v^2 - T(\mathbf{a} \cdot \mathbf{n})^2]\mathbf{I} - \mathbf{P}\mathbf{Q}^c\}\mathbf{e} = \mathbf{0}, \quad \mathbf{P} = \mathbf{I} - \mathbf{a} \otimes \mathbf{a}. \tag{58}$$

This is the propagation condition associated with the single constraint of inextensibility and therefore two waves propagate along the fibre [see Chen and Gurtin (1972)]. Scott (1991) has given an account of the slowness surface of a material that is both incompressible and inextensible. The theory of an elastic solid that is both incompressible and inextensible has achieved wide currency as a model for fibre-reinforced materials in which an incompressible matrix is reinforced by inextensible fibres [see e.g. Spencer (1972)]. We shall often refer to such an idealized fibre-reinforced material as an IFRM.

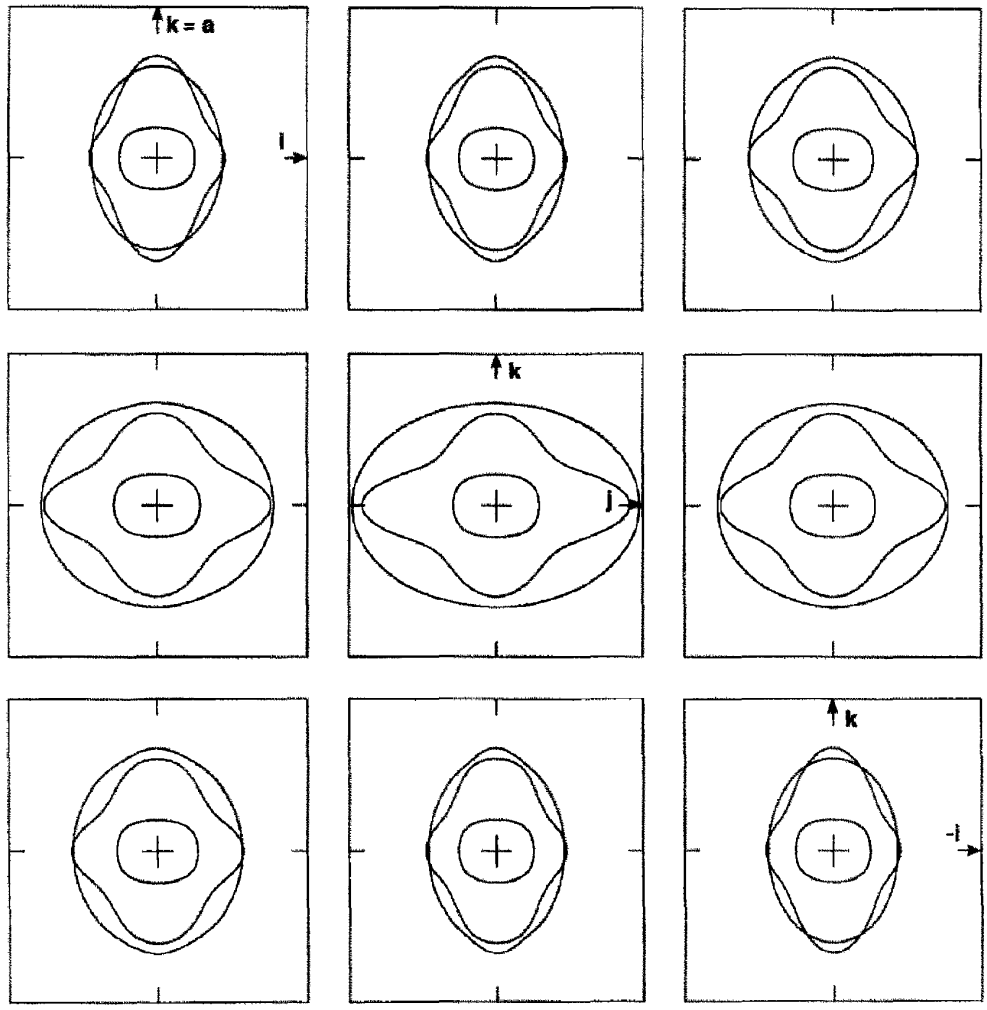

Fig. 3(a). Cross-sections of the slowness surface of a fairly incompressible, fairly inextensible elastic material: $c_1 = 1$, $c_2 = 0.14$, $\kappa = 10$, $E = 10$; $\lambda_1 = \frac{3}{2}$, $\lambda_2 = \frac{2}{3}$, $\lambda_3 = 1$.

6.2. *Cross-sections of the slowness surface of a nearly incompressible, nearly inextensible elastic solid*

It was observed in the previous section that in general a single plane wave is able to propagate in an incompressible, inextensible elastic solid. In addition to this general case there are two exceptional cases, namely, propagation along and propagation normal to the fibre direction, in each of which cases two plane waves are able to propagate. In this section these constraints are relaxed and cross-sections of the slowness surface are presented in an attempt to elucidate the nature of these singularities. The strain energy function used for purposes of illustration is the modified Mooney–Rivlin form

$$W = c_1(J_1 - 3) + c_2(J_2 - 3) + \tfrac{1}{2}\kappa(J-1)^2 + \tfrac{1}{8}E(J_4 - 1)^2, \tag{59}$$

in which c_1 and c_2 are positive constants, κ is essentially the bulk modulus, E is essentially the Young's modulus along the direction of near-inextensibility and J_1, J_2 and J_4 are invariants of $\mathbf{C}$ defined by

$$J_1 = \operatorname{tr}\mathbf{C}, \quad J_2 = \tfrac{1}{2}\{(\operatorname{tr}\mathbf{C})^2 - \operatorname{tr}(\mathbf{C}^2)\}, \quad J_4 = \mathbf{A}\cdot(\mathbf{CA}). \tag{60}$$

For convenience we shall often refer to the direction of near-inextensibility as the fibre

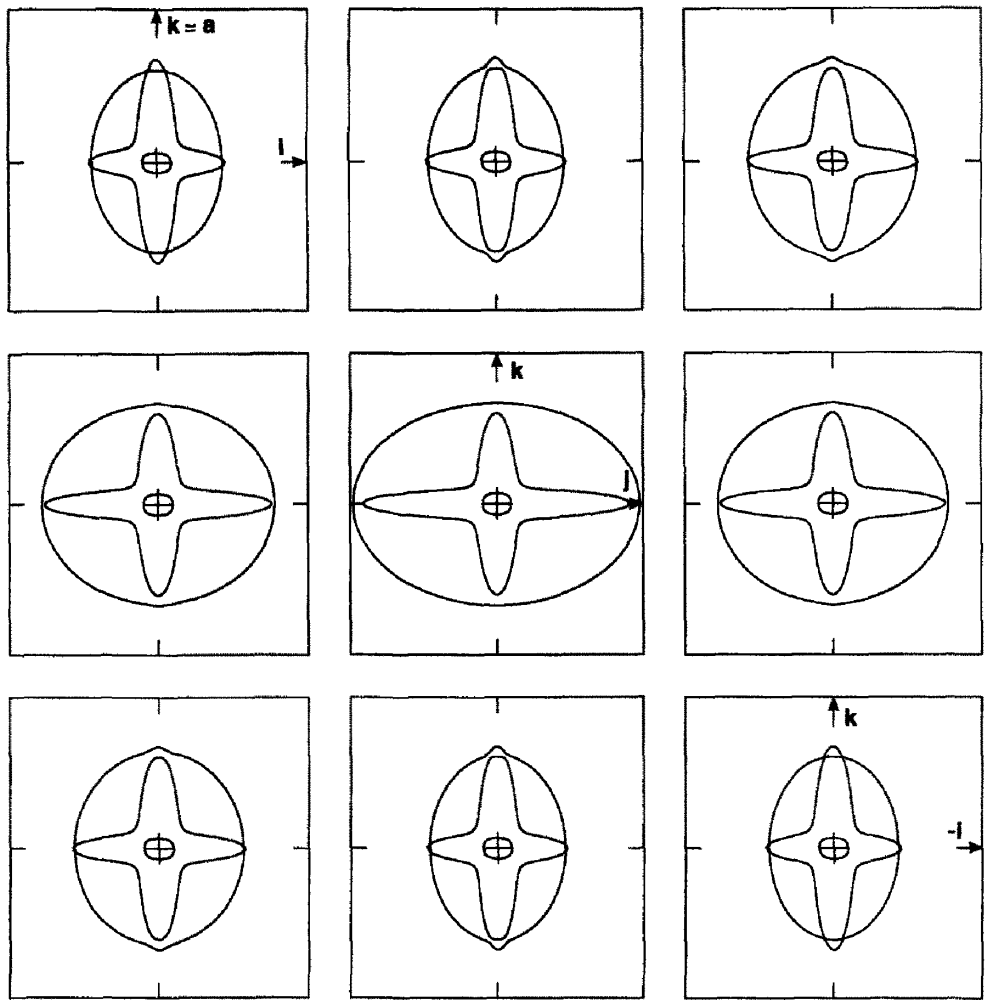

Fig. 3(b). Cross-sections of the slowness surface of a nearly incompressible, nearly inextensible elastic material: $c_1 = 1$, $c_2 = 0.14$, $\kappa = 100$, $E = 100$; $\lambda_1 = \frac{3}{2}$, $\lambda_2 = \frac{2}{3}$, $\lambda_3 = 1$.

direction. The mechanical model for fibre-reinforced materials has become one in which a nearly incompressible matrix is reinforced by nearly inextensible fibres.

The bulk modulus and Young's modulus play the same role as $c^{[1]}$ and $c^{[2]}$ in the general theory discussed in Section 5. As $\kappa \to \infty$, $E \to \infty$, $J-1 \to 0$ and $J_4-1 \to 0$, the material approaches the doubly constrained IFRM limit. We shall now present cross-sections of the slowness surface of a nearly incompressible, nearly inextensible elastic solid. The Cartesian coordinate system is based on the principal axes $\{\mathbf{i}, \mathbf{j}, \mathbf{k}\}$ of the left Cauchy–Green strain tensor [see eqn (1)] so that

$$\mathbf{B} = \lambda_1^2 \mathbf{i} \otimes \mathbf{i} + \lambda_2^2 \mathbf{j} \otimes \mathbf{j} + \lambda_3^2 \mathbf{k} \otimes \mathbf{k}, \tag{61}$$

where λ_i $(i = 1, 2, 3)$ are the principal stretches. In each of Figs 1–4 a series of nine cross-sections of a three-sheeted slowness surface is presented, each containing the **k**-axis which in all cases is drawn vertically. The first cross-section in each set shows the $(\mathbf{i}, \mathbf{k})$ plane, the next showing 22.5 degree rotation about the **k**-axis so that the fifth cross-section is in the $(\mathbf{j}, \mathbf{k})$ plane and the ninth is a reflection of the first in the vertical axis.

In Figs 1–3 cross-sections of the slowness surface of a nearly incompressible, nearly inextensible elastic solid are depicted. In each cross-section the fibre direction is parallel to the **k**-axis.

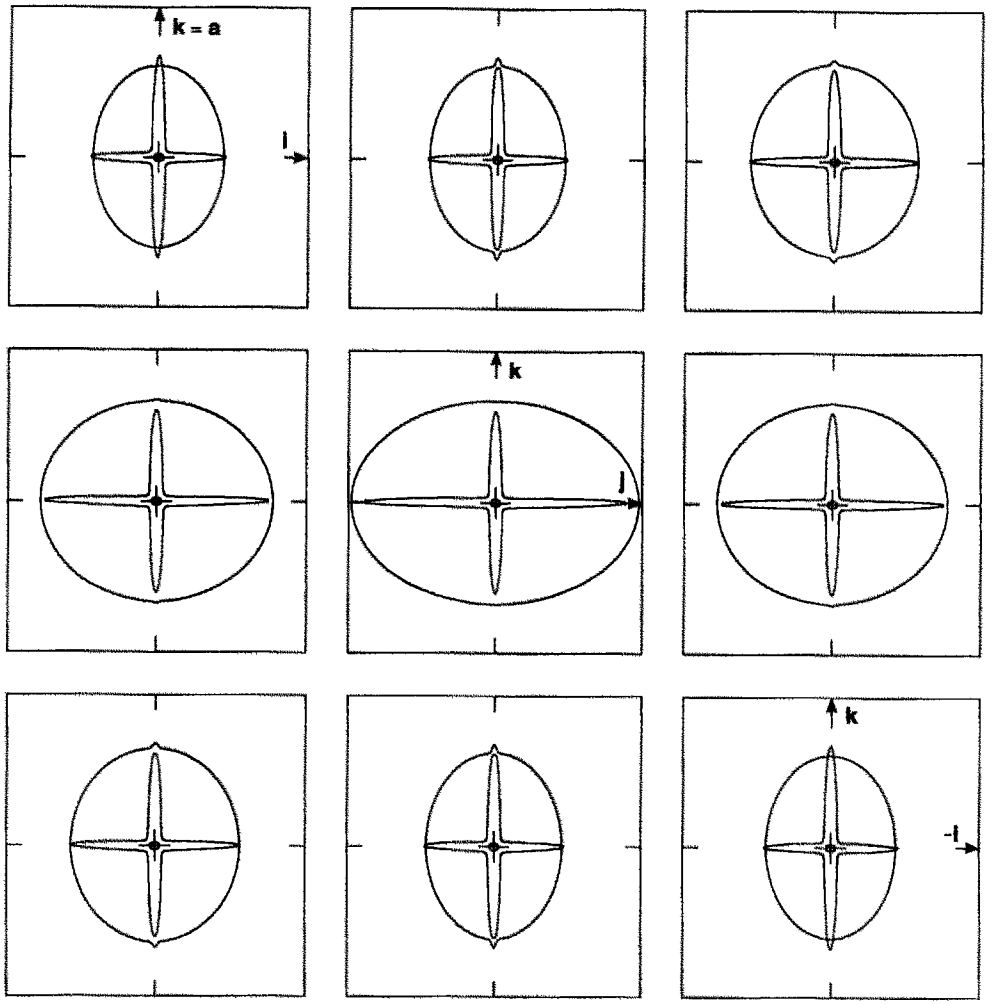

Fig. 3(c). Cross-sections of the slowness surface of a virtually incompressible, virtually inextensible elastic material: $c_1 = 1$, $c_2 = 0.14$, $\kappa = 1000$, $E = 1000$; $\lambda_1 = \frac{3}{2}$, $\lambda_2 = \frac{2}{3}$, $\lambda_3 = 1$.

In Fig. 1 the material is virtually incompressible and nearly inextensible in the sense that the bulk modulus ($\kappa = 1000$) is much larger than the Young's modulus ($E = 200$) though both are much greater than the other elastic constants ($c_1 = c_2 = 1$). The innermost sheet appears to be a small sphere centred on the origin and detached from the two outer sheets. This behaviour exemplifies that of the innermost sheet of the slowness surface of a nearly incompressible material [see Scott (1986)]. The passage to the limit of incompressibility is remarkably well illustrated by comparing the present Fig. 1 with Fig. 10 of Scott (1992b) for a strictly incompressible, nearly inextensible material having precisely the same elastic moduli and prestrain as in Fig. 1 except that in Scott (1992b), incompressibility means that κ is effectively infinite. The two outer sheets of Fig. 12 are apparently the same as the two sheets of Fig. 10 of Scott (1992b) for each cross-section; the small sphere of the former figure has shrunk to the origin in the latter because of incompressibility. Rogerson and Scott (1992a, Figs 4 and 5) illustrate that the more inextensible a material becomes, the more parts of the slowness surface come to resemble a disc with normal parallel to the fibre direction. The present Fig. 1 also illustrates this phenomenon for the fibre direction $\mathbf{a} = \mathbf{k}$. Cross-sections of the disc are apparent in each part of the figure mainly as part of the middle sheet of the slowness surface. In addition, our Fig. 1 illustrates the formation of a spike along the fibre direction which is due to a combination of incompressibility and inextensibility. This spike collapses to a line segment parallel to the fibre direction in the

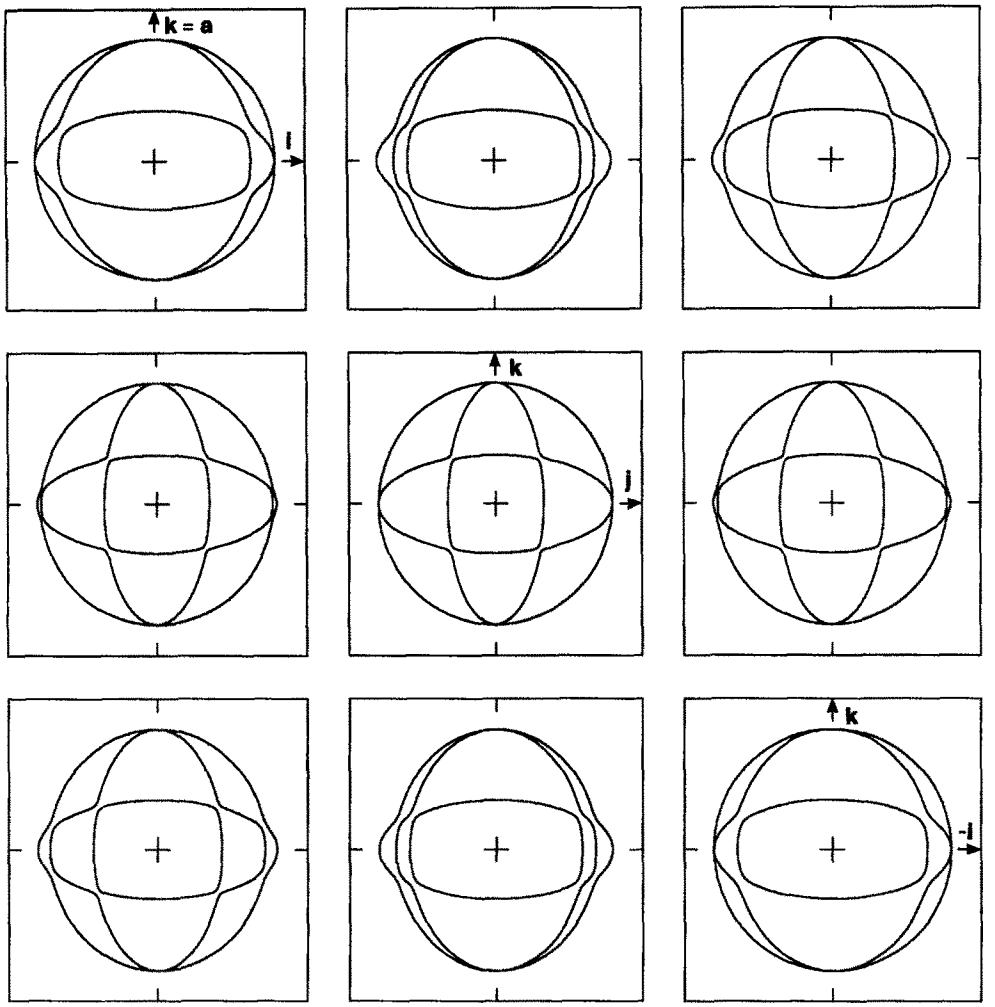

Fig. 4(a). Cross-sections of the slowness surface of an unstrained elastic material reinforced by two orthogonal sets of fairly inextensible fibres: $c_1 = 1$, $c_2 = 0.14$, $\kappa = 1$, $E = 10$, $E' = 10$.

IFRM limit. The one-sheeted slowness surface of the doubly constrained IFRM has been discussed by Scott (1991). That author has also elucidated the nature of the spike singularity along the fibre direction [see Scott (1992b, Fig. 16)], and the disc singularity normal to the fibre direction [see Scott (1992b, Fig. 19)], by considering wave propagation in an incompressible, nearly inextensible material.

The slowness surface cross-sections depicted in Fig. 2 are for a fairly incompressible, nearly inextensible material in (a) and for a fairly incompressible, virtually inextensible material in (b). They are to be compared with Fig. 2 of Rogerson and Scott (1993) for a fairly incompressible, strictly inextensible material having precisely the same elastic moduli and prestrain as in the present Fig. 2(a) except that in Rogerson and Scott (1993) inextensibility means that E is effectively infinite. Both parts of the present Fig. 2 clearly illustrate the formation on the slowness surface of a disc whose normal is parallel to the direction $\mathbf{k} = \mathbf{a}$ of the nearly inextensible fibres. The disc is much flatter in Fig. 2(b) because the Young's modulus is much larger than in Fig. 2(a). There is no such disc present in the two-sheeted slowness surface of the strictly inextensible material depicted in Fig. 2 of Rogerson and Scott (1993); there the disc has collapsed completely onto the $(\mathbf{i}, \mathbf{j})$ plane because of inextensibility and so is not apparent in any cross-section containing the fibre direction $\mathbf{k}$. Even for the small admixture of incompressibility present in our Fig. 2, we see that in (a) the innermost sheet is detached from the other two, as in Fig. 1, and that (a) and (b) both display the beginnings of the spike in the fibre direction, clearly apparent

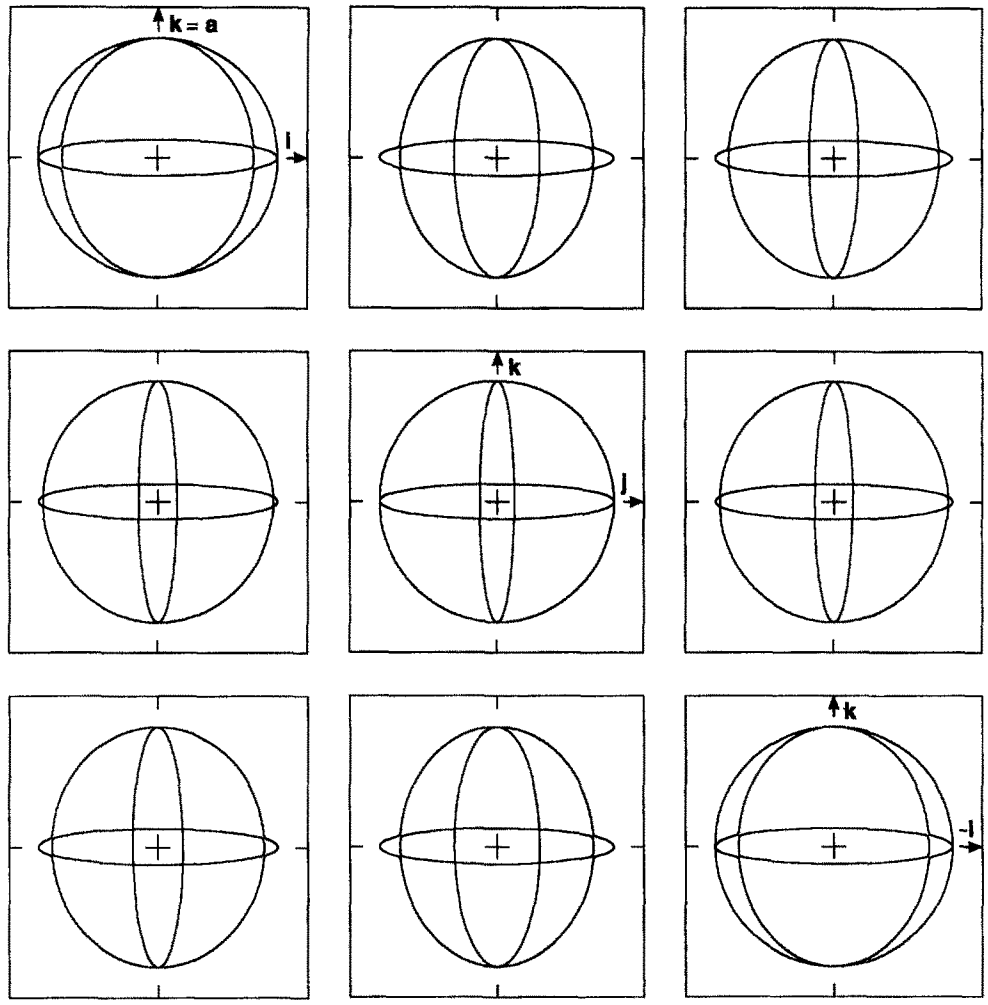

Fig. 4(b). Cross-sections of the slowness surface of an unstrained elastic material reinforced by two orthogonal sets of nearly inextensible fibres: $c_1 = 1$, $c_2 = 0.14$, $\kappa = 1$, $E = 100$, $E' = 100$.

in Fig. 1, that results from the material being both nearly incompressible and nearly inextensible.

In Fig. 3 the effects of near-incompressibility and near-inextensibility are roughly comparable with neither predominating over the other contrasting with Figs 1 and 2. This is achieved by taking the bulk and Young's moduli to be equal in each part of the figure. In Fig. 3(a) we have taken $\kappa = E = 10$ so that the effects of the near-constraints are quite moderate. Even so, the innermost sheet is detached and the beginnings of a disc perpendicular to the fibre direction and of a spike parallel to the fibre direction may just be discerned. The effects of increasing the degree of inextensibility whilst maintaining the same degree of incompressibility may be ascertained from a comparison of Figs 2(a) and 3(a); the disc and the spike become more pronounced in Fig. 2(a) with increasing inextensibility and the innermost sheet becomes decidedly less spherical, though remaining detached from the others, as near-incompressibility plays a subordinate role. In Fig. 3(b) we have taken $\kappa = E = 100$ so that the effects of the two near-constraints are much more noticeable than in Fig. 3(a); the detached innermost sheet is smaller and more nearly spherical whilst the approximate disc and spike are more pronounced. These effects are even more strikingly apparent in Fig. 3(c) where the choice $\kappa = E = 1000$ renders the constraints virtually exact. This figure is to be compared with Fig. 3 of Rogerson and Scott (1993) depicting the two-sheeted slowness surface of a virtually incompressible, strictly inextensible material in which the disc normal to the fibre direction is absent because of inextensibility but the spike along the fibre direction remains.

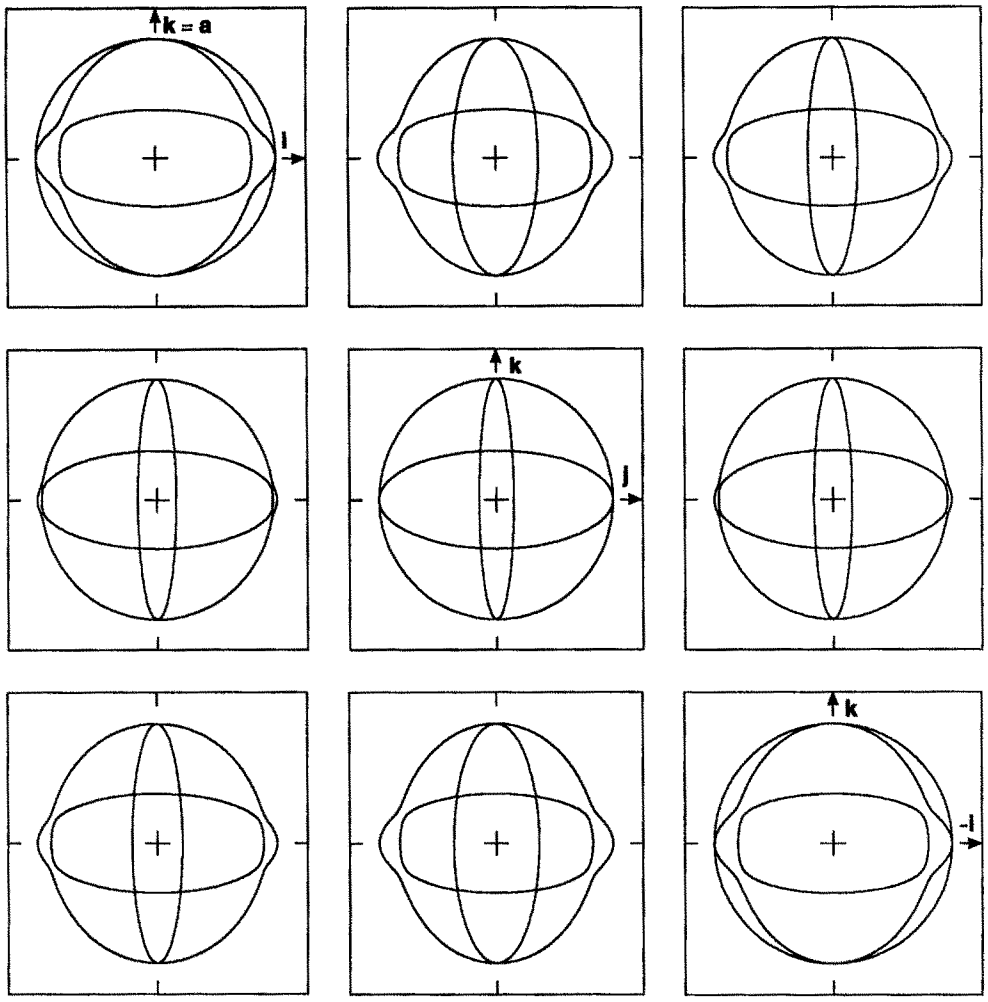

Fig. 4(c). Cross-sections of the slowness surface of an unstrained elastic material reinforced by two orthogonal sets of nearly inextensible fibres: $c_1 = 1$, $c_2 = 0.14$, $\kappa = 1$, $E = 10$, $E' = 100$.

To summarize the effects of increasing incompressibility and inextensibility we observe from Fig. 3 that the outer sheet of the slowness surface undergoes little change as the values of κ and E become larger. This sheet is the sheet which corresponds to the single sheet of the IFRM slowness surface. In Fig. 3(c) the behaviour of the outer sheet both near the fibre and close to directions normal to it indicates clearly that the associated wave speed is discontinuous in the limit of exceptional directions. The middle sheet of the slowness surface exhibits the most rapid change as the IFRM limit is reached. As κ and E are increased, this sheet becomes a thin disc perpendicular to the fibre with a thin spike normal to this disc and so along the fibre. In the IFRM limit this sheet becomes a disc of zero thickness normal to the fibre with two line segments along the positive and negative directions of the fibre. This sheet then guarantees that two waves (rather than one) propagate along the fibre and in every direction normal to the fibre direction, i.e. in each exceptional direction.

6.3. *Two sets of inextensible fibres*

Consider now two sets of inextensible fibres whose directions in B_e are given by $\mathbf{a}$ and $\mathbf{b}$, respectively. The appropriate results from Section 6.1 may now be used in conjunction with eqn (18) to deduce that the appropriate propagation condition takes the form

$$(\mu\mathbf{I}-\mathbf{Q}^c)\mathbf{e}-T_a^*(\mathbf{a}\cdot\mathbf{n})\mathbf{a}-T_b^*(\mathbf{b}\cdot\mathbf{n})\mathbf{b}=\mathbf{0}, \quad \mathbf{a}\cdot\mathbf{e}=0, \quad \mathbf{b}\cdot\mathbf{e}=0, \tag{62}$$

in which

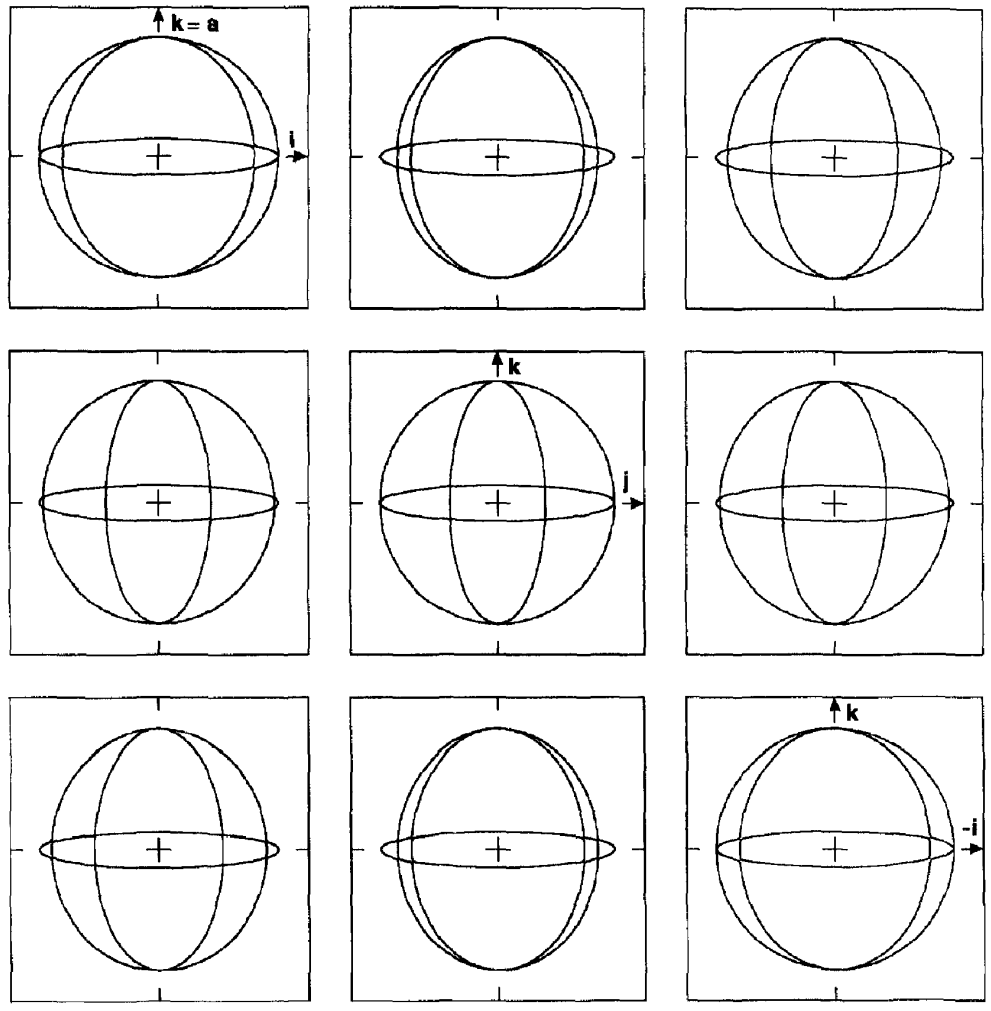

Fig. 4(d). Cross-sections of the slowness surface of an unstrained elastic material reinforced by two orthogonal sets of nearly inextensible fibres: $c_1 = 1$, $c_2 = 0.14$, $\kappa = 1$, $E = 100$, $E' = 10$.

$$\mu = \rho v^2 - \{T_a(\mathbf{a}\cdot\mathbf{n})^2 + T_b(\mathbf{b}\cdot\mathbf{n})^2\},$$

and the subscripts a and b indicate arbitrary tensions along **a** and **b**, respectively. It is readily deduced that a single plane wave is able to propagate in each non-exceptional direction. The wave speed and polarization vector can easily be found by analysis similar to the general analysis of Section 3.1.

In the first exceptional case to be discussed, namely those directions for which $\mathbf{a}\cdot\mathbf{n} = 0$, the propagation condition may be written as

$$\{[\rho v^2 - T_b(\mathbf{b}\cdot\mathbf{n})^2]\mathbf{I} - \mathbf{Q}^c\}\mathbf{e} = 0, \quad \mathbf{b}\cdot\mathbf{e} = 0. \tag{63}$$

This is the propagation condition appropriate for waves propagating in an elastic solid with a single set of inextensible fibres in the direction **b** [see e.g. Chen and Gurtin (1972)]. A similar conclusion is arrived at in the case $\mathbf{b}\cdot\mathbf{n} = 0$. It is then concluded that two plane waves are able to propagate in any direction for which either $\mathbf{a}\cdot\mathbf{n} = 0$ or $\mathbf{b}\cdot\mathbf{n} = 0$. In conclusion we note from eqn (62) that if both $\mathbf{a}\cdot\mathbf{n} = 0$ and $\mathbf{b}\cdot\mathbf{n} = 0$, the propagation condition is then exactly that associated with the unconstrained problem [see eqn (6)].

6.4. *Cross-sections of the slowness surface of an elastic body reinforced by two sets of perpendicular, nearly inextensible fibres*

In this section the propagation of waves through an elastic material reinforced by two sets of perpendicular, nearly inextensible fibres is discussed. The two fibres are taken to be perpendicular in B_e with directions **a** and **b**, respectively. For purposes of illustration the strain energy function is again taken in a modified Mooney–Rivlin form

$$W = c_1(J_1-3)+c_2(J_2-3)+\tfrac{1}{2}\kappa(J-1)^2+\tfrac{1}{8}E(J_4-1)^2+\tfrac{1}{8}E'(J_6-1)^2, \qquad (64)$$

in which $J_6 = \mathbf{B}\cdot(\mathbf{CB})$ (here **B** denotes the fibre direction $\mathbf{F}^{-1}\mathbf{b}$ measured in B_u), E' is effectively the Young's modulus along the fibre direction **b** and all other parameters are as defined for eqn (59). If the two Young's moduli are equal ($E = E'$), the two sets of fibres are said to be mechanically equivalent.

As $E \to \infty$, $E' \to \infty$, $J_4 - 1 \to 0$ and $J_6 - 1 \to 0$, the material approaches the limit of an elastic solid reinforced by two sets of inextensible fibres. In order to examine this limit and try to elucidate the singularities which occur for the constrained solid, we present cross-sections of the slowness surface. The coordinate system is that employed in Section 6.2 with one of the fibre directions parallel to **k** and the other parallel to **j**. From Figs 4(a) and (b) it is observed that in the case of mechanically equivalent fibres ($E = E'$), the innermost sheet of the slowness surface collapses to a straight line along the direction normal to both fibres, i.e. the **i**-direction. In the limit $E = E' \to \infty$, an examination of this sheet shows that the only finite wave speed associated with it is in a direction normal to both fibres.

As the value of $E = E'$ is increased, the middle sheet of the slowness surface tends to two discs each in a plane perpendicular to one of the fibres. These discs have zero thickness in the limit of two inextensible fibres. The existence of these discs implies that it is only perpendicular to each fibre that there exists a finite wave speed in the limit associated with the middle sheet. The rapid changes along and perpendicular to the fibres can also be seen on the other cross-sections. The fifth section, showing the (**j**, **k**) plane, in each of Figs 4(a) and (b), shows the plane containing both fibres. In Fig. 4(a) the fifth section shows that in the direction which bisects both fibres the two inner sheets almost touch. This is indicative of a "near-double-point", the existence of which is quite independent of the form of the strain energy function. The high degree of curvature of the slowness surface in the vicinity of the "near-double-point" may well have optical implications connected with conical refraction.

On comparing the outer sheets of Figs 4(a) and (b) we find that they change very little as $E = E'$ increases. As $E = E' \to \infty$, this outer sheet tends to the single sheet of the slowness surface of a material reinforced by two perpendicular sets of inextensible fibres.

Figure 4(b) is to be compared with Fig. 2 of Rogerson and Scott (1991). The latter figure also relates to a material reinforced with two perpendicular sets of nearly inextensible fibres but there the material is, in addition, nearly incompressible so that the inner sheet is detached from the other two.

The remaining parts of Fig. 4 depict a situation in which the fibres in one direction are much less extensible than those in the other. In Fig. 4(c) the fibres in the **j**-direction are much more nearly inextensible ($E' = 100$) than those in the **k**-direction ($E = 10$). In consequence the approximate discs in the (**i**, **k**) plane (relating to the **j**-fibres) is much thinner than that in the (**i**, **j**) plane (relating to the **k**-fibres). In Fig. 4(d) the roles of the two sets of fibres are reversed ($E = 100$, $E' = 10$) so that now the approximate disc in the (**i**, **j**) plane is much thinner than that in the (**i**, **k**) plane.

7. CONCLUSIONS

In each of Figs 1–4 the behaviour of the slowness surface indicates a high degree of material anisotropy. This anisotropy is associated with the different exceptional directions which occur in the limit. It was seen in Section 3.2 that three distinct classes of exceptional direction occur in a doubly constrained solid. This number increases as the number of

constraints is increased, e.g. seven distinct classes occur in an elastic solid subject to three constraints [see Rogerson and Scott (1991)]. It is well known that the direction of energy propagation is normal to the slowness surface. Therefore, the high degree of curvature of the slowness surface of a multi-constrained elastic material, as apparent from Figs 1–4, indicates likely singular behaviour of the energy flux vector in the constrained limit. This interesting possibility has been commented upon previously by the present authors [see Rogerson and Scott (1992b)] who, in the case of a limited class of singly constrained boundary value problems, have shown that the magnitude of the energy flux vector tends to zero in the constrained limit. Chadwick *et al.* (1985) and Scott (1992a) have also discussed energy propagation. A more detailed analysis of energetics associated with multi-constrained wave problems, however, remains lacking at the present time.

REFERENCES

Beatty, M. F. and Hayes, M. A. (1992a). Deformations of an elastic, internally constrained material. Part I: homogeneous deformations. *J. Elasticity* **29,** 1–84.

Beatty, M. F. and Hayes, M. A. (1992b). Deformations of an elastic, internally constrained material. Part 2: nonhomogeneous deformations. *Q. J. Mech. Appl. Math.* **45,** 663–709.

Bell, J. F. (1985). Contemporary perspectives in finite strain plasticity. *Int. J. Plasticity* **1,** 3–27.

Bell, J. F. (1989). Experiments on the kinematics of large plastic strain in ordered solids. *Int. J. Solids Structures* **25,** 267–278.

Chadwick, P. (1976). *Continuum Mechanics, Concise Theory and Problems*. George Allen and Unwin, London.

Chadwick, P., Whitworth, A. M. and Borejko, P. (1985). Basic theory of small amplitude waves in a constrained elastic body. *Arch. Rat. Mech. Anal.* **87,** 339–354.

Chen, P. J. and Gurtin, M. E. (1972). On wave propagation in inextensible elastic bodies. *Int. J. Solids Structures* **10,** 275–281.

Ericksen, J. L. (1986). Constitutive theory for some constrained elastic crystals. *Int. J. Solids Structures* **22,** 951–964.

Fu, Y. B. (1993). On the stability of inextensible elastic bodies: nonlinear evolution of non-neutral, neutral and near-neutral modes. *Proc. R. Soc. London* **443,** 59–82.

Green, W. A. (1978). Wave propagation in strongly anisotropic elastic materials. *Arch. Mech.* **30,** 297–307.

Musgrave, M. J. P. (1970). *Crystal Acoustics*. Holden-Day, San Francisco.

Rogerson, G. A. and Scott, N. H. (1991). Wave propagation in exceptional directions in multi-constrained elastic solids. *Int. J. Engng Sci.* **29,** 1337–1348.

Rogerson, G. A. and Scott, N. H. (1992a). Wave propagation in singly constrained and nearly constrained elastic materials. *Q. J. Mech. Appl. Math.* **45,** 77–99.

Rogerson, G. A. and Scott, N. H. (1992b). Aspects of energy propagation in highly anisotropic elastic solids. *Acta Mech.* **92,** 129–141.

Rogerson, G. A. and Scott, N. H. (1993). Singly constrained elastic wave propagation and the limit of two constraints. *Wave Motion* **18,** 291–302.

Scott, N. H. (1975). Acceleration waves in constrained elastic materials. *Arch. Rat. Mech. Anal.* **58,** 57–75.

Scott, N. H. (1986). The slowness surface of incompressible and nearly incompressible elastic materials. *J. Elasticity* **16,** 239–250.

Scott, N. H. (1991). Small vibrations of prestrained constrained elastic materials: the idealized fibre-reinforced material. *Int. J. Solids Structures* **27,** 1969–1980.

Scott, N. H. (1992a). Plane waves in twinned crystals modelled as multi-constrained and nearly constrained elastic materials. *J. Mech. Phys. Solids* **40,** 1607–1619.

Scott, N. H. (1992b). Waves in a homogeneously prestrained incompressible, almost inextensible fibre-reinforced material. *Proc. R. Ir. Acad.* **92A,** 9–36.

Spencer, A. J. M. (1972). *Deformations of Fibre-reinforced Materials*. Clarendon Press, Oxford.

Stewart, I. W. and Raj, N. (1990). Application of continuum smectic C theory to alignment inversion walls. *Molec. Cryst. Liquid Cryst.* **185,** 47–59.

Truesdell, C. and Noll, W. (1965). The non-linear field theories of mechanics. In *Handbuch der Physik* Vol. 3/III. Springer, Berlin.

Willson, A. J. and Myers, P. J. (1990). The radial motions of elastic shells. *Int. J. Engng Sci.* **28,** 1235–1243.